

## Derailment in track switches

*Master's Thesis in the Applied Mechanics Programme*

**MARTIN ANDERSSON**

Department of Applied Mechanics

*Division of Dynamics*

CHALMERS UNIVERSITY OF TECHNOLOGY

Göteborg, Sweden 2012

Master's thesis 2012:22



MASTER'S THESIS IN APPLIED MECHANICS

# Derailment in track switches

MARTIN ANDERSSON

Department of Applied Mechanics  
*Division of Dynamics*  
CHALMERS UNIVERSITY OF TECHNOLOGY  
Göteborg, Sweden 2012

Derailment in track switches  
MARTIN ANDERSSON

© MARTIN ANDERSSON 2012

Master's Thesis 2012:22  
ISSN 1652-8557  
Department of Applied Mechanics  
Division of Dynamics  
Chalmers University of Technology  
SE-412 96 Göteborg  
Sweden  
Telephone: + 46 (0)31-772 1000

Cover: Picture of a train vehicle model from GENSYS software

Chalmers Reproservice  
Göteborg, Sweden 2012

## ABSTRACT

The European project D-RAIL aims at reducing the occurrences and impacts of freight train derailments, improving the understanding of the causes behind derailment and anticipating derailment through measurement of appropriate system parameters. The objective is to account for underlying causes of derailment and their interactions effects.

The derailment risk of freight train traffic needs to be quantified. In this parametric study a total of 17 parameters are included and evaluated in a two-level design of experiments (DOE). In the DOE a response variable is used as a measure of the derailment risk. The response variable is the  $Y/Q$ -ratio of the wheel- rail forces, where  $Y$  is the lateral force and  $Q$  the vertical force. The simulation model is made in the multi-body dynamics software GENSYs.

13 of the parameters are vehicle based and focus on the friction in the damping surfaces, stiffness of the primary and secondary suspensions etc. whilst the non-vehicle based parameters address track irregularities, gauge distance and so forth.

First the DOE 1, containing eight parameters, is used to exclude three parameters controlling the stiffness of the centre pivot. Nine additional parameters are then used in a larger, DOE 2 where the result shows that the largest  $Y/Q$ -ratio value obtained is 1.35, so the limit value according to Nadal is exceeded with about 0.5. The effects are presented in a normal probability plot. The most significant effects prove to be related both to the vehicle and the track.

Key words: parametric study, design of experiments, multi-body dynamics, normal probability plot, derailment, switch, turnout

Utspårning i spårväxlar  
Examensarbete inom Tillämpad Mekanik  
MARTIN ANDERSSON  
Institutionen för tillämpad mekanik  
Avdelningen för Dynamik  
Chalmers tekniska högskola

## SAMMANFATTNING

För det europeiska samarbetsprojektet D-RAIL är målet att reducera antalet utspårningar för godstrafik. Detta kan uppnås genom ökad förståelse av orsakerna bakom utspårning samt att kunna förutse utspårning genom att mäta viktiga systemparametrar.

Utspårningsrisken för godståg måste kvantifieras. I denna studie inkluderas och utvärderas totalt 17 olika parametrar i två-nivåsfaktor försök. I faktor försöket används  $Y/Q$ -kvoten som respons variabel för att mäta utspårningsrisken, där  $Y$  är lateral kontaktkraft mellan hjul och räl och  $Q$  motsvarande vertikal kraft.

Simuleringsmodellen är skapad i flerkroppsdynamikprogramvaran GENSYS.

13 av parametrarna är fordonsparametrar och fokuserar bland annat på friktionskoefficienter i dämpningsytorna i primär och sekundärfjädringarna etc. De fyra icke-fordonsparametrarna riktar sig till rälojämnheter, spårvidd och så vidare.

Ett litet faktor försök med åtta parametrar används för att kunna sortera bort tre parametrar som styr styvheten i centrumpannan. Nio ytterligare parametrar inkluderas sen i ett, 14-parameter, stort faktor försök där resultaten visar på en  $Y/Q$ -kvot på 1.35 jämfört med gränsvärdet på 0.8 utan att någon utspårning äger rum. Effekterna från de olika parametrarna visas i ett normalfördelningsdiagram. De mest signifikanta effekterna visar sig tillhöra både fordon- och rälparametrar.

Nyckelord: utspårningsrisk, faktor försök, flerkroppsdynamik, GENSYS,  $Y/Q$ -kvot, normalfördelningsdiagram

# Contents

1	INTRODUCTION	5
2	THEORY	6
2.1	Design of experiments	6
2.2	Railway systems	7
2.3	Vehicle coordinate system	8
2.4	The Y25 bogie	9
2.5	Turnouts	11
2.6	Derailment criteria	11
3	PARAMETERS	14
3.1.1	Primary suspension friction damping surfaces	14
3.1.2	Damping and stiffness in the secondary suspension	14
3.1.3	Friction coefficient in the centre pivot	15
3.1.4	Sidebearer play	15
3.1.5	Axle load	16
3.1.6	Bogie C-C distance	16
3.1.7	Wheel profiles	17
3.1.8	Load distribution	18
3.1.9	Suspension stiffness	18
3.1.10	Suspension tweak	19
3.1.11	Gauge distance	19
3.1.12	Twisted track	20
3.1.13	Hanging sleeper	20
3.1.14	Turnout entry	21
4	SIMULATION SETUP	22
4.1	DOE 1	22
4.2	DOE 2	22
4.3	Dynamic train-turnout interaction	23
5	DOE 1	24
5.1	Results	24
5.1.1	DOE 1	24
5.1.2	Result from setup 1	26
5.1.3	Result setup 2	28
5.1.4	Result setup 3	29
5.1.5	Result setup 4	31
5.2	Conclusions DOE 1	32
6	DOE 2	33

6.1	Results DOE 2	33
6.1.1	Result setup 5	34
6.2	Conclusions	36
7	DERAILMENT LIMIT	38
7.1	Derailment limit results	39
7.2	Derailment limit conclusions	40
8	FUTURE WORK	42
9	SUSTAINABLE DEVELOPMENT	43
10	BIBLIOGRAPHY	44

## **Preface**

I would like to thank my supervisor Björn Pålsson (Licentiate of Engineering) at the Department of Applied Mechanics at Chalmers University of Technology, for his patience with me and my many questions in my effort of trying to grasp all the areas of theory behind the subjects in this thesis. He has been my tireless support and guidance during this project. I would also like thank my examiner Professor Jens C. O. Nielsen, at the same department for his inspiring manner and thorough attention.

Thanks to the personnel at SWEMAINT for their explanations regarding the mechanics of the Y25 bogie and to Igor Antolovic at Kockums Industries AB for sending me pictures of the Y25 bogie.

Göteborg in June 2012

Martin Andersson

## Notations

$a_y$	Lateral acceleration
$\beta$	Flange angle
$R$	Turnout radius
$Y$	Lateral wheel-rail contact force
$Q$	Vertical wheel-rail contact force
$L_2$	c-c distance between bogies in a wagon

## Abbreviations

DOE	Design of Experiments
EN	European Standards
UIC	Union Internationale des Chemins de Fer, International Union of Railways
$Y/Q$	Lateral to vertical wheel rail contact force ratio, used as a derailment criterion
Y25	Freight train bogie type

# 1 Introduction

Railway transport is an important part of the competitive transport sector where restrictions on polluting emissions are becoming more and more comprehensive. The railway traffic is however sensitive to disturbances, so it is important to maintain vehicles and infrastructure to ensure reliability.

With the deregulation of train operation and track maintenance in Europe, it is becoming increasingly more important that maintenance limits are well-defined and based on a scientific approach. This is even more the case when dealing with potential safety-critical aspects. In order to strengthen the position of railways in the competition for freight transport, it is necessary to understand what factors are crucial for derailment.

The objective of the EC-project D-rail is to reduce the occurrences and impacts of freight train derailments. In this work, the influence on derailment risk for freight traffic in turnouts from 14 traffic parameters is calculated using design of experiment (DOE) methods. The response criterion and indicator of derailment risk used is the ratio of lateral and vertical force ( $Y/Q$ ) in the wheel rail contact. The  $Y/Q$ -ratio for each parameter setting is evaluated using simulations of vehicle-turnout interaction in the multi body dynamics software GENSYS [1]. A model of a freight car with Y25 bogies is chosen as representative for freight traffic in Europe.

The derailment limit used in this project is the  $Y/Q$ -ratio set to 0.8. Some studies claim this value to be conservative and low, instead suggesting 1.2 as a more realistic value [2].

A brief derailment experiment is performed to investigate the impact from the worst case scenario setup, obtained as a result from the second DOE. Three friction parameters, the speed and the centre of gravity (COG) are varied within chosen intervals. This will provide derailment limit guidelines.

## 2 Theory

The theory described below can be found in G E P Box, J S Hunter and W G Hunter, *Statistics for experimenters 2<sup>nd</sup> edition*, John Wiley & Sons Inc., New Jersey, 2005 [4]. The basics can be found in U Blomqvist, *Försöksplanering - Faktorförsök*, Matematiklitteratur, 2003.

### 2.1 Design of experiments

A design of experiments (DOE) or factorial design is a way of planning experiments so that it is possible to obtain main effects as well as higher order effects for different factors by changing their values in a predetermined pattern. Just changing one value at the time would not expose all possible effects. By the use of a DOE, all effects can be studied and interactions, perhaps unexpected, can be revealed. A number of factors, which are known or believed to affect the result, are included in the experiment and are assigned a high and a low value. The values are referred to as levels, and are symbolized by +1 and -1. To measure the influence of each factor, a response criterion is needed. A demonstration example of a two-factor DOE is shown in Table 1. The columns A and B represent the factors A and B. In run one both the factors are set to their low value or level, -1. The resulting response criterion, column Y, shows the value 17. This table or matrix shows all the combinations possible for two factors with two levels, a two to the power of two DOE.

Table 1 Example DOE with a result table for two factors

Run number	A	B	AB	Result, Y
1	-1	-1	+1	Y <sub>1</sub> =17
2	+1	-1	-1	Y <sub>2</sub> =26
3	-1	+1	-1	Y <sub>3</sub> =14
4	+1	+1	+1	Y <sub>4</sub> =19

The effect associated with a certain factor is calculated as the difference between the average result of the high and low levels in the DOE. Using the example in Table 2, the main effect for factor A can be calculated as:

$$l_A = l_{A^+} - l_{A^-} = \frac{y_2 + y_4}{2} - \frac{y_1 + y_3}{2} = \frac{26 + 19}{2} - \frac{17 + 14}{2} = 7 \quad (1)$$

For a full factorial design, the total number of interactions for a  $k$ -factor,  $N$ -level, experiment is:

$$\text{Interactions of all orders} = N^k - 1 - k \quad (2)$$

A large, full factorial design can be time consuming as the number of experiments grows exponentially with the number of factors.

$$\text{Total number of experiments for a full factorial design} = N^k \quad (3)$$

Therefore a full factorial design with a large number of factors is not very effective. Instead a so called fractional factorial design can be utilised where the number of runs is reduced to:

$$\text{Number of experiments for a fractional factorial design} = N^{k-p} \quad (4)$$

where  $p$  is the number of independent generators which is required for each level of reduction. An independent generator is a factor that is confounded with, preferably, a third or higher order interaction which is not likely to be relevant. It is not possible to distinguish the effect from a certain factor if it is confounded with another, instead it will be the sum of the effects from the two (or more) factors that is calculated. Confounding is the cost for reducing the number of experiments. For example, a  $2^{5-2}$  design will require two independent generators. Depending on how the generators are chosen in a fractional factorial design the confounding pattern, or alias, varies.

Example: Consider for the two generators:  $E=BCD$  and  $F=ABCD$ , one three-way and one four-way interaction, in a  $2^{6-2}$  factorial design. The generating relations:  $I_1=BCDE$  and  $I_2=ABCDF$  will give the third generating relation  $I_3=I_1 * I_2=BCDE * ABCDF = AEF$ . In general, if there is an even amount of factors present, those factors can be removed ( $AABBCD=CD$  or  $B * B=I$  etc.) as  $-1 * -1=1$ . In this case,  $I_3$  contains three letters and the DOE is therefore of resolution three. This resolution means that no confounding is present between main effects, but the main effects are confounded with two-way effects. If instead the generators are chosen as:  $E=ACD$  and  $F=BCD$ , two three-way interactions, with the generating relations  $I_1=ACDE$ ,  $I_2=BCDF$  and  $I_3=I_1 * I_2=ABEF$  will produce a DOE with the resolution four.

A  $2^6$  full factorial design would have needed 64 runs, but after the reduction it only needs 16 runs and becomes a  $2_{IV}^{6-2}$  DOE. The resolution  $IV$  states that no confounding is present between main effects and two-way effects but the two-way interaction effects become confounded with each other. The resolution in this study is set to  $V$ , which means that no confounding occurs between main factors or the two-way interactions effects [3] [4].

As the current thesis work is based on simulations with absolute repeatability, it is straightforward to determine significant effects, according to the simulation model, as there are no measurement errors.

## 2.2 Railway systems

There is railway traffic all over the world carrying people or cargo to their destinations. The railway tracks can be divided into different systems, i.e. Gothenburg has tramways which is a system integrated with the road network and connects the suburb to the city. Other cities, like Stockholm, the capital of Sweden, has subways or metros that are mostly running underground in its own system, separated from other kinds of traffic. Further, there is the traditional railway that connects cities and countries, carrying both people and freight traffic.

It is possible to divide rail vehicles into two classes; powered vehicles or coaches and wagons. The powered vehicles are usually driven by diesel or electricity. Rail vehicles consist of two main parts, the running gear and the carbody. Included in the running gear are the wheels, axles and suspensions. The carbody contains the passenger seats or the cargo bay.

## 2.3 Vehicle coordinate system

The six degrees of freedom for rail vehicles are shown in Table 2 below and illustrated in Figure 1, [5].

Table 2 Degrees of freedom in rail vehicle dynamics [5].

Relative motions	Symbol	notation
Translation in direction of travel	$x$	Longitudinal
Translation in transverse direction, parallel to the track plane	$y$	Lateral
Translation perpendicular to the track plane	$z$	Vertical
Rotation about a longitudinal axis	$\varphi$	Roll
Rotation about a transverse axis, parallel to the track plane	$\kappa$	Pitch
Rotation about an axis perpendicular to the track plane	$\psi$	yaw

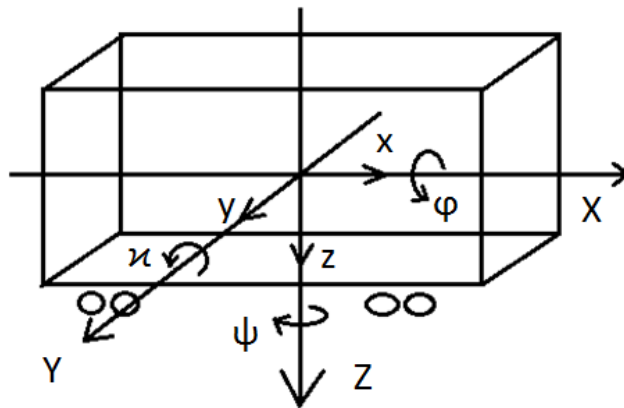


Figure 1 Relative motion for the vehicle, components according to Table 2. Adapted from [5]

A nominal or static condition describes a vehicle at rest on a perfect plane and a tangent track. When a vehicle runs at constant speed in a curve with constant radius and constant cant and wheel-rail contact, it is said to be in a quasistatic condition (accelerations are constant). This is an idealized condition, only achievable in simulations, where all forces and relative displacements are constant in time. In more realistic situations, for example when the track is not perfect, the forces and relative motion are time dependent and in a so called dynamic condition [5].

## 2.4 The Y25 bogie

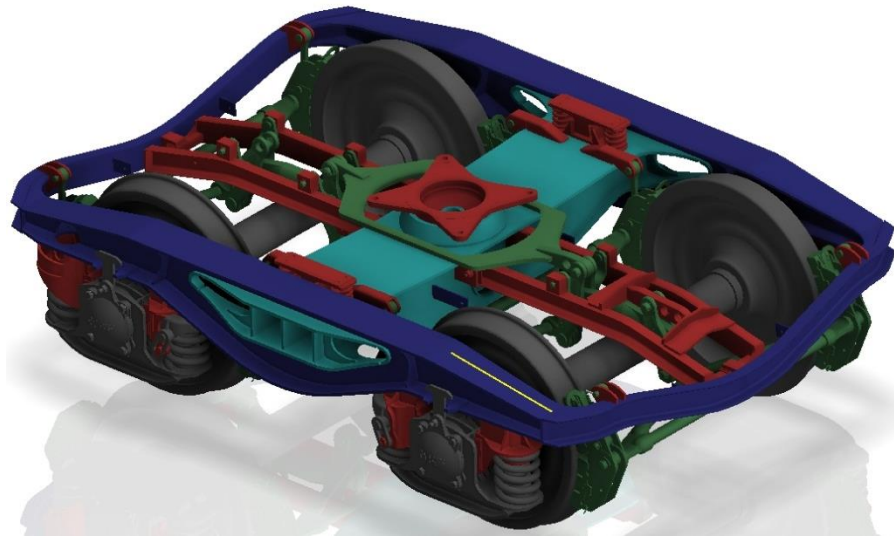
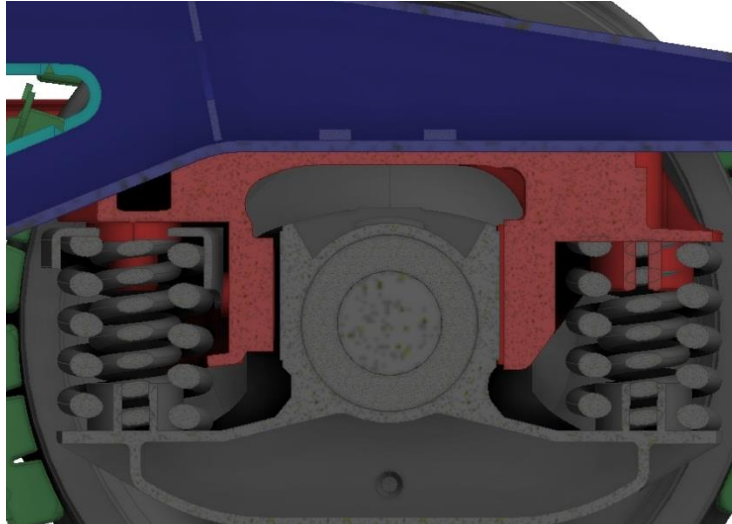


Figure 2 A Y25 bogie made by Kockums industries AB. Picture from Kockums Industries AB

The running gear of a rigid-frame vehicle only consist of one wheelset and the suspension components at each end of the vehicle, while the bogie vehicles has one or more wheelsets, a framework and the suspension components [5]. In this thesis the simulations are based on a model with Y25 bogies [6]. No investigation will be made of the rigid frame arrangements.

The Y25 bogie is shown in Figure 2. The Y25 bogie is a standard UIC design [5] and is a so called “heavy transport wagon”. It can carry a maximum axle load of 25 tons when travelling at speeds up to 100 km/h. The construction consists of two side beams, one transverse beam and two end beams. A very stiff centre pivot is attached on the transverse beam and this is the point of interaction between carbody and bogie together with the two side bearers that help carry the load. The distribution of the load in the tare case is 38% on the side bearers and 90% in the loaded case [6].

The primary suspension consists of a total of 16 coil springs, eight for each axle. They connect the hornguides on the outer ends of the two side beams to the axle boxes. On each side of the axle boxes there are two springs The smaller spring is only in use when the wagon is carrying load [5] [6]. The arrangement is shown in Figure 3. The suspension consists not only of coil springs but also of damping surfaces. The damping is achieved by friction between surfaces. In the primary suspension, there are six different friction surfaces for each axle box.



**Figure 3** The coil springs in the primary suspension. Two sets of springs, the smaller inner spring and the larger outer spring. The left and right sets are called: “in towards” and “out from” bogie centre [6]. Picture from Kockums Industries AB

The normal load on the axle box friction surfaces is a fraction of the load in the primary springs providing cargo-load dependent damping. The load is transferred via a pusher. The load is due to the inclination of the Lenoir link which allows the top of the coil spring to move longitudinally and apply pressure on the pusher. The Lenoir link is highlighted in Figure 4.

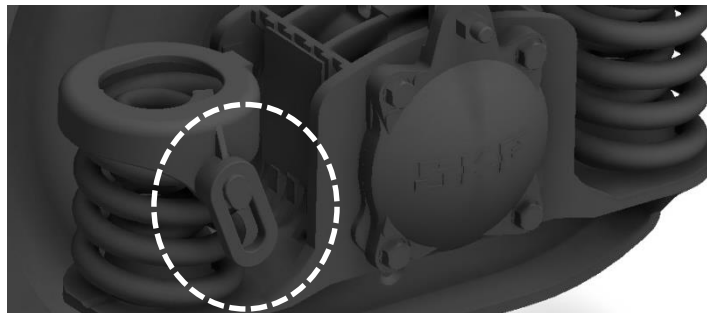


**Figure 4** The Lenoir link makes the damping load-dependent as it applies pressure on “the pusher” that forces the axle boxes against the corresponding surfaces on the frame. Picture from Kockums Industries AB

The sidebearers are included in the secondary suspension. They have dedicated friction surfaces which allow friction damping in the X-Y plane and Y-Z plane, see Figure 1 for plane illustrations. The secondary suspension also includes the centre pivots.

In total there are 26 friction surfaces on the bogie including the centre pivot, eight in the Y-Z plane, 16 in the X-Z plane and two in the X-Y plane [6]. The friction coefficient in the centre pivot is lower than the sidebearer and primary suspension dampers. This is possible because of the centre pivot liner made from reinforced elastomers.

## 2.5 Turnouts

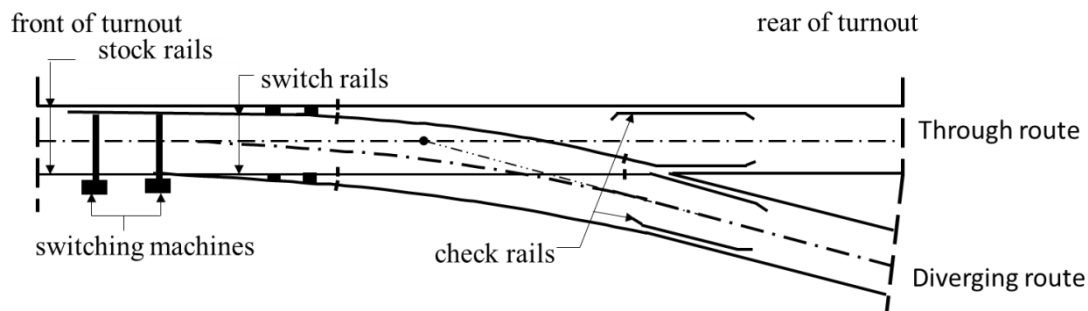


Figure 5 Schematic picture of a turnout, adapted from [7].

A track switch, or turnout, is a track component that allows for trains to change track. A pair of tapered switch rails can be moved laterally by the switching machines to direct the traffic to the through or diverging routes, see Figure 5. In the turnout, large lateral forces may occur between the wheels and switch rail due to complex contact geometry [8].

The most common turnout configuration is a non-symmetric turnout used for connecting a main track to a diverging track. Turnouts stand for 14% of all faults and are the single most common error source in the Swedish railway network [7]. There is about 17000 km of track in Sweden and about 12000 turnouts [8].

The turnout used in this work is a UIC 60E1-190-1:9 with 1:30 rail inclination. The 60E1 specifies the rail profile, the number 190 describes the radius in metres and 1:9 is the turnout angle. The speed is set according to the maximum allowed lateral acceleration according to Deutsche Bahn,  $a_y = 0.654 \frac{m}{s^2}$  where  $a_y = \frac{v^2}{R}$ ,  $v = \sqrt{a_y * R}$

## 2.6 Derailment criteria

A common reason for derailment is flange climbing, it refers to the scenario when the wheel flange climbs onto the top of the rail and continues over the rail head. Flange climbing due to flange steering in under radial position with stiff wheelset guidance and a long wheel base is especially critical. According to Nadal's criterion it is assumed that the angle of attack ( $\alpha$ ), presented in Figure 6, is higher than  $\alpha \geq 0.5^\circ$  so that the lifting force on the flange is pointed almost vertically upwards, as seen in Figure 7. The flange starts to climb when the vertical component of the normal force  $N$  and the friction creep force,  $\mu N$  is larger than the vertical wheel load  $Q$  [5].

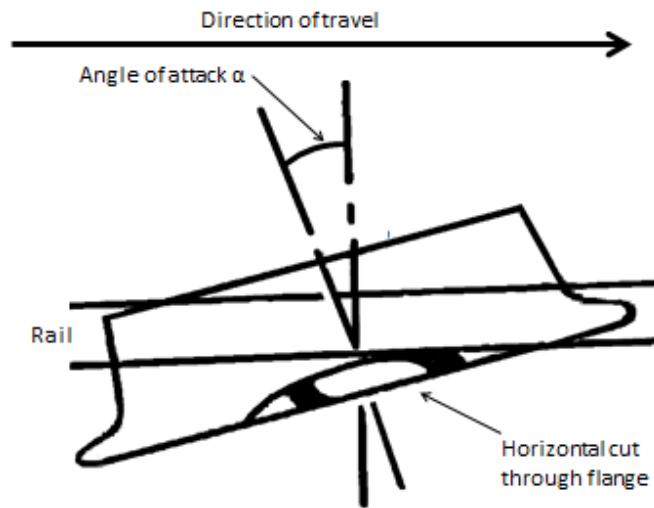


Figure 6 Cut through view showing the angle of attack,  $\alpha$ , in the XY-plane. Adapted from [5]

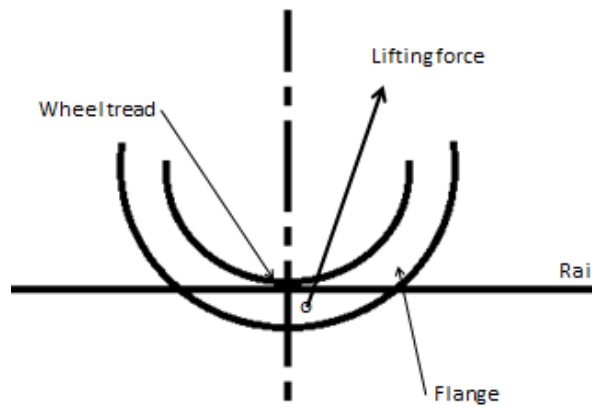


Figure 7 Side view of the wheel, the direction of the lifting force in the XZ-plane. Adapted from [5]

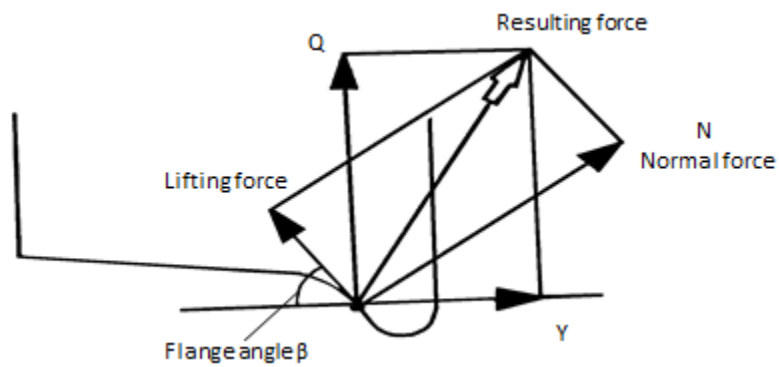


Figure 8 Rear view in the YZ-plane showing the resulting force which can be divided into Y- and Q-forces or lifting forces and normal forces. Adapted from [5]

Nadal's equation describes the relation between  $Y$ ,  $Q$ ,  $\beta$  and  $\mu$  at the start of the flange climbing

$$\left(\frac{Y}{Q}\right)_{Nadal} = \frac{\tan\beta - \mu}{1 + \mu\tan\beta} \quad (5)$$

where  $\beta$  is the flange angle of the wheel and  $\mu$  is the friction coefficient between the wheel and the rail. Depending on the actual relation  $Y/Q$  and  $\mu$ , the flange will climb until the flange angle is large enough to balance the equation. The derailment risk will increase if the flange angle is small and the friction is high.

Permissible  $Y/Q$ -ratio in practice:

$$\frac{Y}{Q} \leq \left(\frac{Y}{Q}\right)_{lim} = A \quad (6)$$

where:  $A=0.8$  for  $\beta=60^\circ$  (worn wheel flange,  $\beta \sim 70^\circ$ ,  $\mu \sim 0.35$  gives  $A=1.2$ )

The International Union of Railways, (UIC), specifies:

$$\left(\frac{Y}{Q}\right)_{lim} = 0.8 \quad (7)$$

for a curve radius larger than 250 meters. The limit value 0.8 originates from the 1970:s and it can be found that: “it was noted that this value was conservative and pessimistic, and it is based on tests simulating extreme conditions”[2]. In this work a 190 meter curve is used in the simulations and perhaps the above mentioned value should have been adjusted for the smaller radius of the track but it still serves the purpose of the study because it will effect on the  $Y/Q$ -ratio from different parameter settings. The standard EN 14363 and UIC518 specifies the limit value as:

$$\left(\frac{Y}{Q}\right)_{20Hz,2m,mean,99,85\%} \quad (8)$$

The 20Hz is indicating that a low pass filter is applied to reduce noise and high sudden loads. A two meter running distance also works as a filter by the use of a two meter floating average that sums up the  $Y/Q$  values within a two meter time dependent interval and divides it by the number of measured steps. It is not the maximum values that is evaluated but the values in the 99.85 percentile. In this work the maximum values of the floating average are used as representative.

### 3 Parameters

The parameters chosen for parameter studies are known or believed to affect the  $Y/Q$ -ratio. They cover different areas such as properties of the Y25 bogie, track irregularities and the vehicle body.

A description of all investigated parameters follows.

Three friction coefficients for damping surfaces are included in the DOE. A friction damper has a nonlinear behaviour and is modelled as a contact surface in series with a linear spring. The spring serves two purposes, it is used for numerical reasons preventing infinite stiffness and the built up force in the spring is used to compare to the friction coefficient multiplied with the normal force,  $\mu * N$ . When the spring force is equal to  $\mu * N$  a motion occurs and energy will be dissipated [5] [6]. The high and low values for the friction coefficients in the damping surfaces are set to 0.1 and 0.5 respectively.

#### 3.1.1 Primary suspension friction damping surfaces

Friction surfaces in the primary suspension are shown in Figure 9. The damping surfaces are located in the hornguides, which are fixed to the frame of the bogie. These damping surfaces are working in the XY and XZ planes of the vehicles coordinate system. The damping works against motions in the directions parallel to these surfaces when the wheel axle moves relative the frame of the bogie. The force applied on the pusher is load dependent and comes, as mentioned above, from the Lenoir link. These contact surfaces are welded on to the underlying frame. According to interviews with the maintenance department at Swemaint AB, the welded plates occasionally crack and need to be repaired.

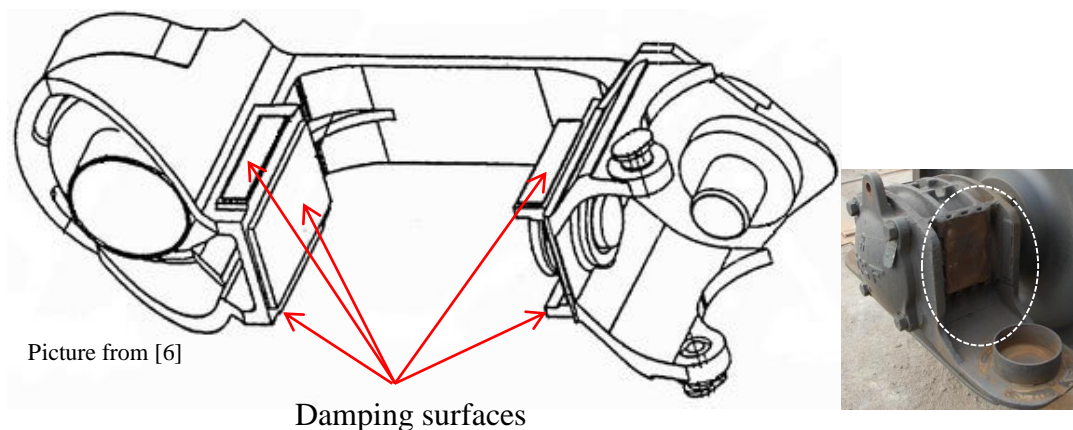


Figure 9 Schematic picture of the damping surfaces in the primary suspension. The left picture shows a hornguide and the right one illustrates an axle box. The damping surfaces are highlighted with arrows and a white dashed oval on the hornguide and the axlebox respectively. Picture from [5]

#### 3.1.2 Damping and stiffness in the secondary suspension

The two sidebearers are located at the left and right sides on the transverse beam in the middle of the bogie together with the centre pivot in the middle, see Figure 10 and Figure 11. Each sidebearer is suspended by two coil springs that support the carbody and the bogie together with the centre pivot. If the vertical displacement of the sidebearers is more than 12 millimetres, the “bottom” of the suspension is reached and

metallic contact occurs. There are three different surfaces on each sidebearer contributing to the damping. The largest surface faces the XY-plane and is in contact with the car body. Two surfaces perpendicular to the large horizontal surface, works as “stop” surfaces in the YZ-plane. They prevent the sidebearers from moving more than a millimetre depending on the initial “play” and the wear of the surface, Figure 12. The larger surfaces in the YX-plane are fixed by screws to the holders but the stop surfaces are welded and experience the same cracking problems as the surfaces in the primary suspension, see Ch. 3.1.1.

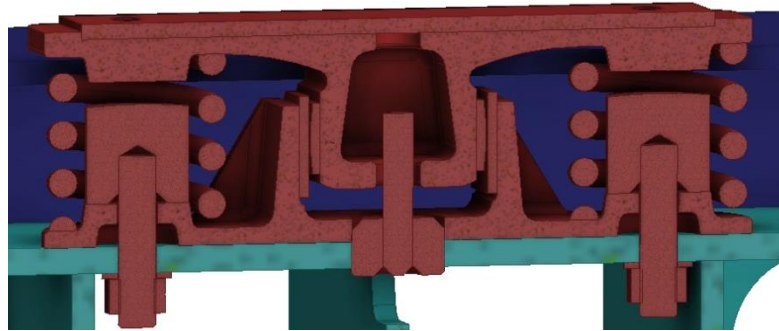


Figure 10 Cut through view of the sidebearer. At the top, the damping surface for contact against the carbody is located, providing friction in the XY-plane. The “play” allows for the sidebearer to move up to a millimetre relative to the stop surface between the two coil springs. Picture from Kockums Industries AB

### 3.1.3 Friction coefficient in the centre pivot

The centre pivot is the only connection joint between the carbody and the bogie. It allows for three-dimensional rotations but no relative translation. This is possible due to a half spherical shaped connection with a centrum screw that holds the carbody and bogie together. A very stiff polymer liner providing friction is placed in between the two metal surfaces of the bogie and the train body. The liner prevents metallic contact and thereby also metallic wear. There is no clearance in the contact so it provides damping in every rotation.

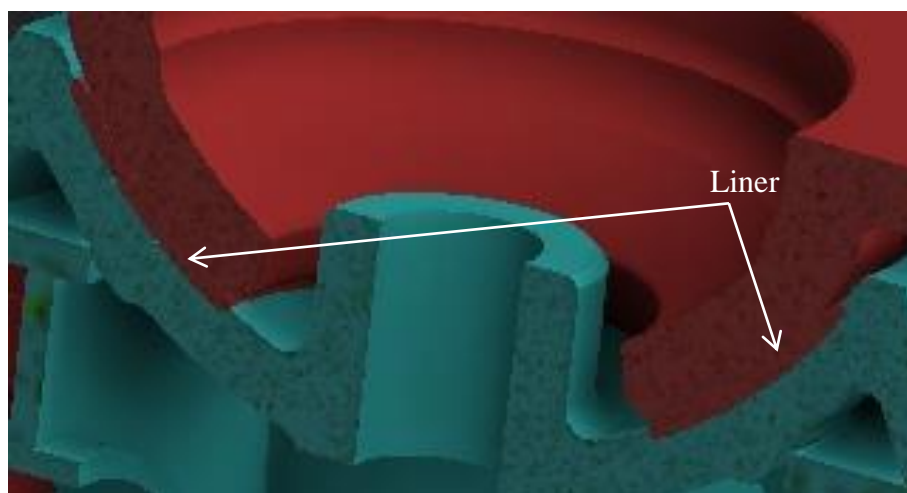


Figure 11 The polymer liner, in the centre pivot, acts as rotational damping surface between the frame of the Y25 bogie and the carbody. Picture from Kockums Industries AB

### 3.1.4 Sidebearer play

The “play” or distance in the sidebearer was mentioned before in the sidebearer section, see Ch. 3.1.2. The “play” between the sidebearer and the sidebearer stops is referring

to the distance that allows the sidebearer to move. The high and low values for the play in the DOE are set to 0.5 and 1.0 millimetres respectively.

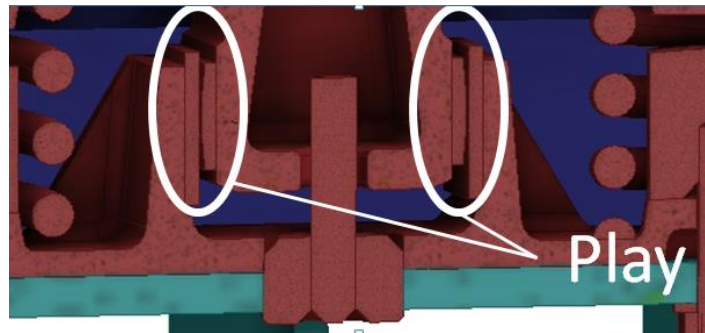


Figure 12 The “play”, between the sidebearer and the stop determines the distance the sidebearer can move. Picture from Kockums Industries AB

### 3.1.5 Axle load

The axle load can vary between the tare case (5 tonnes) and the laden case (25 tonnes). The load distribution parameter, see Ch. 3.1.8, is determined by the axle load.

### 3.1.6 Bogie C-C distance

A survey made of the vehicles equipped with Y25 bogies shows that the Res and the Rs691 or 681 have the longest “L2” length. The L2 length is the centre-centre distance between bogies in a wagon. On these wagons the L2 distance is 15700 [mm]. The Shimmns-g and Shimmns-s wagons have the shortest L2 distance with a L2 distance equal to 7000 [mm] [9].

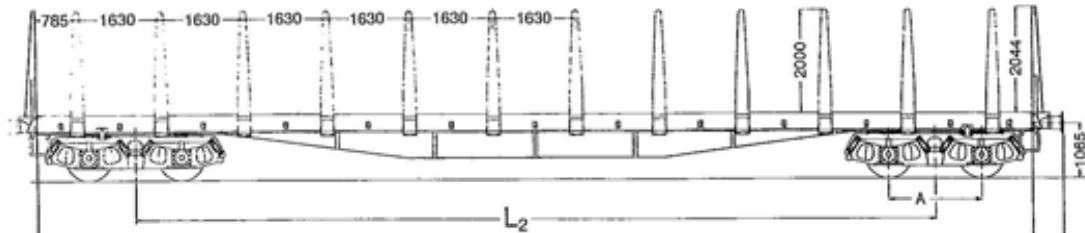


Figure 13 Rs681, L2=15700[mm]. Picture from Green Cargo [9]

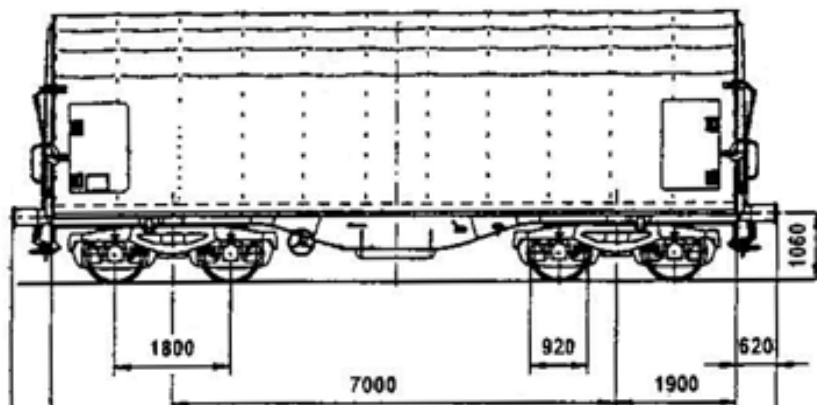


Figure 14 Shimmns-g, L2=7000[mm]. Picture from Green Cargo [9]

These “maximum” and “minimum” lengths are used as the high and low values in the simulations. When changing the L2 distance, the moments of inertia about the Y and Z axes (pitch and yaw) are also changing. The vehicle models used in GENSYS are the same regarding all other parameters except the three mentioned above. The ratio between the long and short carbody is used to determine how large the moment of inertia increase should be. The moments of inertia are scaled in proportion to the length squared.

$$\frac{L_{2_{15.7(long)}}}{L_{2_{7(short)}}} = \frac{15.7}{7.0} = 2.24 \quad (9)$$

In the GENSYS model the carbody is described as a rectangular box. An increase of the length of the carbody will only affect the inertia about the Y and Z axes. The weight of the carbody is set constant for the two different car bodies. In this way it will be the length of the carbody that will be responsible for the change in inertia. The moments of inertia about the Y and Z-axes will increase with linear scaling using Equation (10):

$$\text{Mass moment of inertia} = I = \frac{m * L^2}{12}, \quad I_Y = \frac{m * a^2}{12}, \quad I_Z = \frac{m * b^2}{12} \quad (10)$$

Table 3 Mass moments of inertia for short versus long carbody lengths

Mass moment of inertia	Inertia[kgm <sup>2</sup> ]			
	(Tare case) Short car body	(Tare case) Long Carbody	(Laden case) Short car body	(Laden case) Long carbody
$I_Y = \frac{m * a^2}{12}$	148180	298259	1302800	5080920
$I_Z = \frac{m * b^2}{12}$	151570	305080	13782	5374980

### 3.1.7 Wheel profiles

Two types of wheel profile have been used in the parameter studies. The aim is to reveal differences between a new unworn profile and a used so called “hollow worn” profile. The new profile is represented by a UIC S1002 wheel profile. Looking at the S1002 in a cut through view, the wheel thread has a conical shape that provides the steering capacity. The opposite of the new profile is the “hollow worn” profile which is the result of wear from running on the tracks. The wear is independent of the initial shape of the profile and stabilizes after 100000-200000 kilometres [5]. As the wheel is worn down, the inclination and height of the flange will increase but the conicity will decrease, which can lead to less steering capacity. A worn wheel can be re-profiled to recover its original profile. This is accomplished through milling or by lathe methods and can result in a rough surface which in turn can give high friction between wheel and rail. There have been reports of train vehicles derailling in curves or switches in yards directly after re-profiling [10]. It is not possible in the GENSYS model to replicate a re-profiled

surface but an increased friction coefficient between the wheel and track representing the condition can be modelled.



Figure 15 Wheel profiles, to the left a hollow worn and to the right a new conical shaped wheel, S1002. As seen in the pictures the flange is thinner and the flange angle is larger for the hollow worn profile compared to the new S1002 profile.

### 3.1.8 Load distribution

This parameter describes the distribution of the load of the carbody between the sidebearers and the centre pivot in the secondary suspension. The load distribution is closely connected to the axle load as it's high and low values shift depending on the load the vehicle is carrying. So, when the vehicle is running in the tare case, the low and high values of the load distribution are set to 0.28 and 0.48 respectively. This means that 28% or 48% of the load is carried by the centre pivot and the rest is carried by the sidebearers. In the laden case the low and high values are instead distributed as 75% or 95% on the centre pivot [6]. The two cases are illustrated in Figure 16.

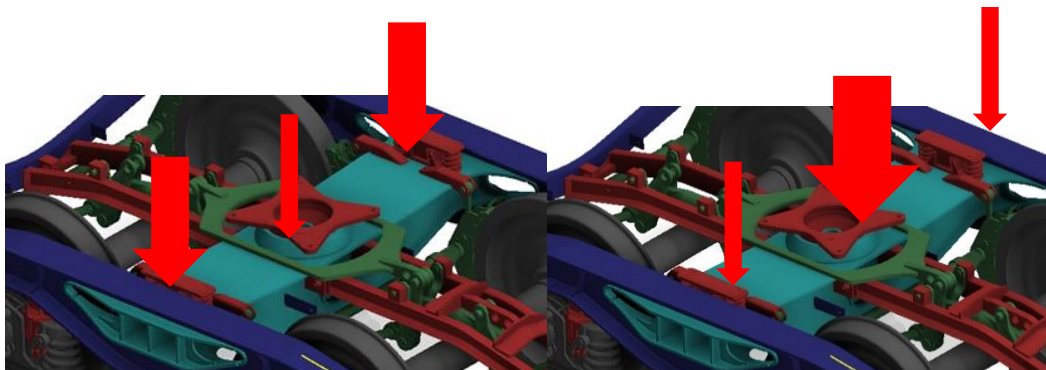


Figure 16 If the axle load is set to the low level, 5 tonnes, the centre pivot carries 28% of the load in the low level and 48% in the high level. If instead the axle load is set to the high level, laden case of 25 tonnes, the low and high levels are set to 75% and 95% respectively. Picture from Kockums Industries AB

### 3.1.9 Suspension stiffness

The different settings for this parameter make it possible to compare a stiffened suspension with a nominal suspension. The increased stiffness addresses the primary suspension on all axles and makes the suspension a hundred times stiffer than the nominal stiffness. This is a way of simulating a “frozen” suspension which could occur on a vehicle that has been used in a cold environment. Snow and ice can accumulate and block the mechanics and prevent the suspension from working correctly. The suspension stiffness is described in three dimensions and the stiffer suspension affects all of them, the yaw, roll and pitch motion of the axles. In a curve-negotiating perspective, this will give the wheelset a larger resistance to yaw, relative the bogie

frame. So when the vehicle enters a curve the wheel will have a larger angle of attack,  $\alpha$ .

The primary suspension has a non-linear behaviour because of the two coil springs, inner and outer, on each side of the axle box. The compression of the outer spring in the primary suspension is maximum 18 millimetres. This leaves a gap between the inner spring and frame of 5 millimetres. When the vehicle is carrying load, enough to compress the outer springs more than the five millimetres, the inner suspension comes in contact with the frame of the bogie and the stiffness gets a non-linear behaviour. This is modelled so only the outer stiffness is present for vertical compression smaller than five millimetres. The sum of the stiffness from both the inner and outer coil springs is used when the vertical displacement (compression) is larger than five millimetres. In the “frozen” case the standard stiffness is multiplied with a factor 100, see Table 4.

**Table 4** The primary suspension has a non-linear behaviour due to the outer and inner springs. The inner, smaller, spring is only in use when the compression of the outer spring is larger than five millimetres. The high and low levels correspond to the “standard” stiffness and a much stiffer “frozen” suspension.

Stiffness of the primary suspension		
Displacement [mm]	5<	<5
Standard stiffness (compression)[N/mm]	2540	9405
“Frozen” suspension (compression)[N/mm]	254000	940500

### 3.1.10 Suspension tweak

The frame of the carbody is modelled as torsionally tweaked by applying different pre-loads on the diagonal of the suspension. One of the pre-loads, lower than the nominal load, is applied on the primary suspensions at the left side of the leading bogie and another pre-load, larger than the nominal load, is applied on the right side. On the following bogie the load pattern is the opposite, see Figure 17.

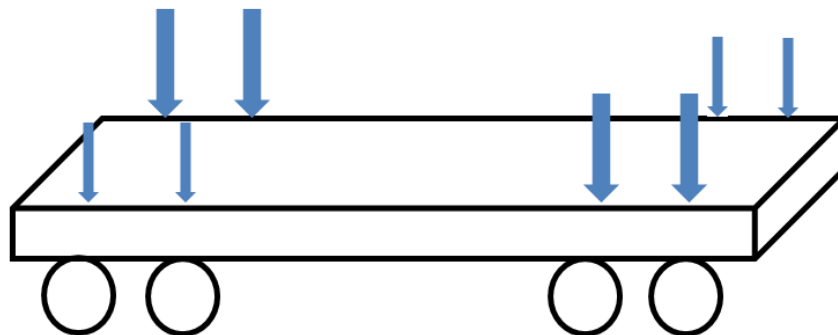


**Figure 17** Diagonally changed preload on the primary suspension.

### 3.1.11 Gauge distance

It is of interest to replicate the reality of the track/rail situation in order to get a realistic simulation. In reality small variations in the track width occurs which could lead to increased risk of flange climb in case of a sudden gauge narrowing. A nominal gauge distance of 1435 millimetres is set as the high level value while the low value corresponds to a gauge narrowing of 10 millimetres to a value of 1425 millimetres, see Figure 18.

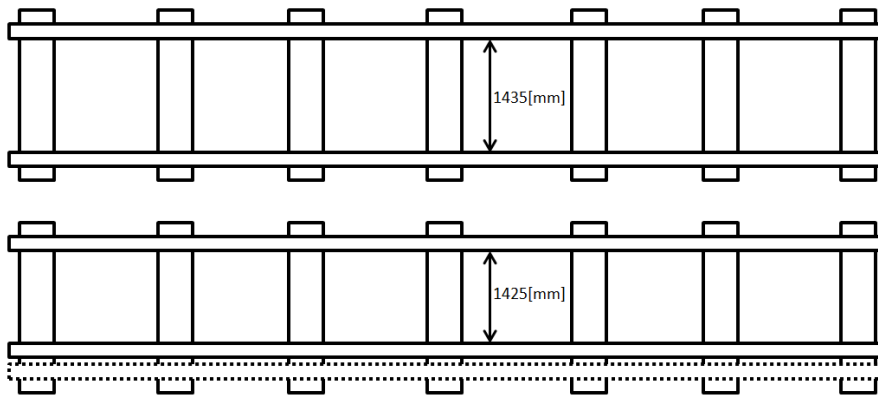


Figure 18 The gauge distance of the track is narrowed by ten millimetres.

### 3.1.12 Twisted track

Twist is the difference in cant between two cross sections of track divided by the distance [5]. The twisted track is a 20 millimetre v-shaped dip in the outer rail of the curve, over a twelve metre span, see Figure 19.



Figure 19 Schematic picture of the 20 millimetre V-shaped track dip used in GENSYS.

### 3.1.13 Hanging sleeper

The sleepers act as support to the rail, and are mainly submerged in ballast. The ballast consists of crushed rock that is packed together by a tamping machine, Figure 20. Occasionally the ballast is disturbed or degraded leading to unsupported sleepers. This affects the stiffness of the track. This is implemented in the GENSYS model with a linear triangulated stiffness described as a “hanging sleeper”, see Figure 21.

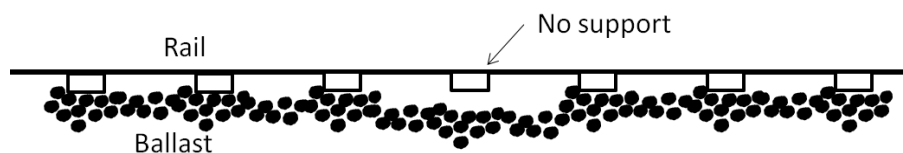


Figure 20 Schematic side view of the track. The sleeper is not supported by the ballast and is just "hanging" in the rail.

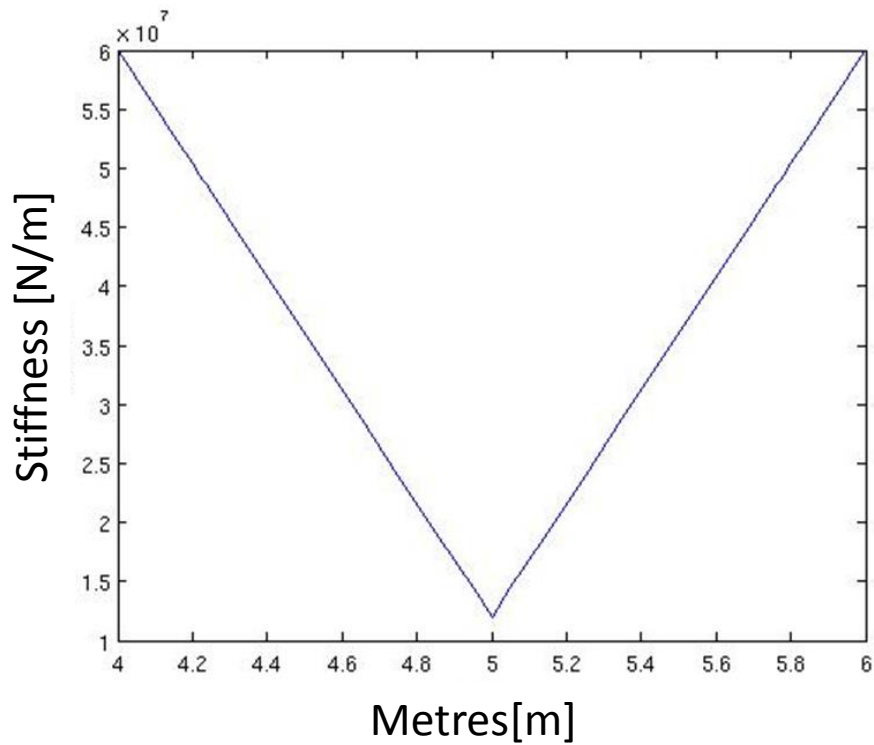


Figure 21 The “loose sleeper” is modelled as a triangulated rail stiffness variation.

### 3.1.14 Turnout entry

There are two different types of turnout entry: tangential entry and radial entry. It describes the track route before the switch. In the tangential entry the switch tongue builds up as a tangent, parallel to the straight track before the radius of the diverging track begins, Figure 23.

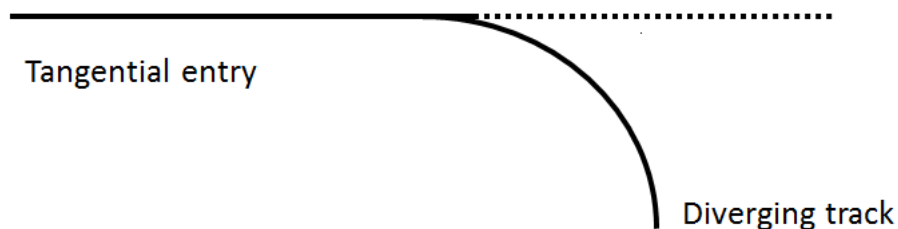


Figure 22 Schematic picture of a curve with the tangential entry.

In the radial entry the switch rail starts to build up within the curvature. High lateral contact forces are present between the wheel and rail as the train negotiates the diverging track, Figure 23.

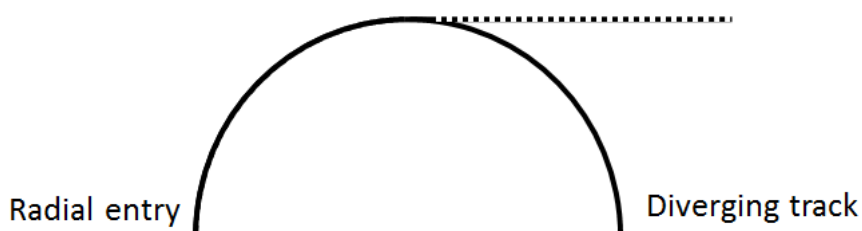


Figure 23 Schematic picture of a curve with a radial entry.

## 4 Simulation Setup

Two DOE's are evaluated covering a total of 17 parameters.

### 4.1 DOE 1

First an eight factor factorial design with resolution five is evaluated, covering only vehicle parameters, see Table 6.

### 4.2 DOE 2

From DOE1 the five most significant parameters are selected and used in the second 14 parameter fractional factorial design, DOE2. The second DOE includes parameters not only related to the Y25 bogie but also to the car body and track irregularities. The second DOE in this experiment is a  $2^{14-6}$  fractional factorial with resolution five. The setup needs six generators in order to obtain resolution five (V). No confounding exists between either the main factors or the two way interactions. The experimental design used here can be found in [11]. Other designs can be found in [4]. It is also possible to find the right generators as described in the chapter "Design of experiments" in this thesis. The factors and aliases can be studied in Table 5 below.

**Table 5 Factors, generators and aliases which are used in the experiment together with some confounding patterns of the effects**

Factor	Generator
1: A	-
2: B	-
3: C	-
4: D	-
5: E	-
6: F	-
7: G	-
8: H	-
9: I	ABCD
10: J	CDEH
11: K	AEFG
12: L	ADGH
13: M	BEFH
14: N	BCFG

However it is clear that the so called letter combination or the defining relation, obtained by multiplying all the generators with each other and removing every quadratic factor, contains at least five letters. This means that the resolution of the experiment is five, or V. A main effect multiplied with one of the generators will produce a defining relation that consists of at least four letters. Similarly, a two-way interaction multiplied with a generator will result in a defining relation with at least three letters. No confounding occurs between main effects or two-way effect which is preferred as it would not be able to separate which one of the factors that is accountable for the effect.

A  $2_V^{14-6}$ , fractional factorial design, requires 256 runs. The design matrix is created in Matlab using the statistical toolbox function called “*fracfact*”.

From the input string generator, which consists of the letters symbolizing each of the factors that are included in the experiment, the outputs are the design matrix and the confounding pattern. The design matrix uses 1 and -1 to represent each factor’s high and low values. The sign, in the column for the interactions, is the product of the factors from the same row that are included in the interaction. In total it is possible to get  $2^{14} - 1 = 16383$  different effects from a full two-level DOE with 14 parameters, but the effects from interactions of higher order than two are likely to be small and are therefore not considered in this evaluation. The number of two-way interaction effects in this experimental design can be calculated as [12]:

$$\binom{14}{2} = \frac{14!}{2! * (14 - 2)!} = \frac{14!}{2! * 12!} = \frac{14 * 13}{2} = 91 \quad (11)$$

Together with the 14 main effects it adds up to a total of 105 effects evaluated in this experiment.

The pre-processing has been performed in Matlab. All the settings are stored and loaded in to an “*optif*”-file in the simulation software GENSYS. These files determine the pattern for every run of the GENSYS model, and calls for the “*tsim*”-file which contains the GENSYS model. The parameters changes values according to the *optif*-file and the runs are performed automatically and are stored as Matlab “*m*”-files through the “*cataf*” output file.

The output from GENSYS is loaded into Matlab by the use of the “*eval*” command and the data necessary is saved into vectors. The lateral and vertical forces are filtered with a 20 Hz low-pass, fourth order Butterworth filter to reduce the level of disturbing noise.

Finally the *Y/Q*-ratio is calculated using a floating average, where the average is calculated over a two metre distance. The maximum value from each run is used as response variable. The maximum values are used to calculate the effects and presented in a normal distribution probability plot to show the result from the experiment.

The *Y/Q*-ratio is used as derailment risk criterion but it does not tell whether an actual derailment has taken place. The *Y/Q*-ratio can exceed the limit value 0.8 without derailment. A derailment criterion is created that measures the lateral displacement of a bogie axle. If the displacement surpasses a given threshold, a derailment has taken place.

### 4.3 Dynamic train-turnout interaction

The train-turnout interaction for a given parameter setting is evaluated using the commercial MBS-code GENSYS.

The train model used in this work is the same as in [8], paper F. It is validated for ordinary traffic in turnouts and will give reasonable *Y/Q*-ratio estimates. However, the model is not tested and validated for wheel climb scenarios, which is expected in a derailment scenario caused by flange climb in a turnout. The focus is to find the parameter(s) that triggers the flange climb and results in a high *Y/Q*-ratio.

## 5 DOE 1

For the DOE 1, eight parameters are used as a screening to see if all of them are necessary to include in a larger DOE 2. All of the parameters are vehicle parameters and are shown in Table 7. The parameters include three friction parameters, three stiffness parameters, load distribution and a distance or “play” within the sidebearers as presented in Section 3.

Table 6 The eight different factors evaluated in the first, small, experiment.

Factor	Description	Low level	High level
A:	Friction coefficients for primary suspension	0.1	0.5
B:	Friction coefficient for side bearers	0.1	0.5
C:	Friction coefficient for centre pivot	0.1	0.5
D:	Play: distance between side bearer friction surface and boarders	0.5[mm]	1[mm]
E:	Stiffness in centre pivot X-direction	0.20e6[Nm]	0.10e7[Nm]
F:	Stiffness in centre pivot Y-direction	0.20e6[Nm]	0.10e7[Nm]
G:	Stiffness in centre pivot Z-direction	0.20e6[Nm]	0.10e7[Nm]
H:	Load distribution between side Bearer and centre pivot*	0.28/0.75[%]	0.48/0.95[%]

\*If the run is made as a tare case, 5 tonnes, the low and high levels of the load distribution are set to 28% and 48% between the centre pivot and the sidebearers respectively. In the loaded case, 25 tonnes, the low and high levels are set to 0.75% and 0.95%.

### 5.1 Results

The results from this study are quantified with a low pass filtered, two meter floating average of the  $Y/Q$ -ratio, see Section 4. The  $Y$  and  $Q$  forces are the lateral and vertical wheel rail contact forces respectively. In the normal distribution plot (normplot) the main effects and the interaction effects are studied. The runs are separated with different, randomly selected colours.

The normplot shows the effect a certain setting of the parameters has on the response value ( $Y/Q$ -ratio). The probability for the response value is plotted on the Y-axis. The effect the factor or the interaction has on the response value is plotted on the X-axis, see Figure 24.

All effects that follow a normal distribution will be located on a straight line in the normal distribution plot. Significant effects will be located to the left or right side of the straight line which is the normal distribution, see Figure 26, [13][4].

#### 5.1.1 DOE 1

It is concluded from the experiments that main factors A, B, C, D and H repeatedly have the largest effects. Some interaction effects between the same factors are also present. The first result is from a smaller screening using eight vehicle based parameters, evaluated for four different combinations of radius, speed and axle load. These can be studied together with their high and low values in Figure 24 and Table 7 below.

Table 7 The setup used for the four different simulations in DOE 1.

Setup	Turnout radius[m]	Load[ton]	Speed[km/h]
1	760	5	80
2	760	25	80
3	190	5	40
4	190	25	40

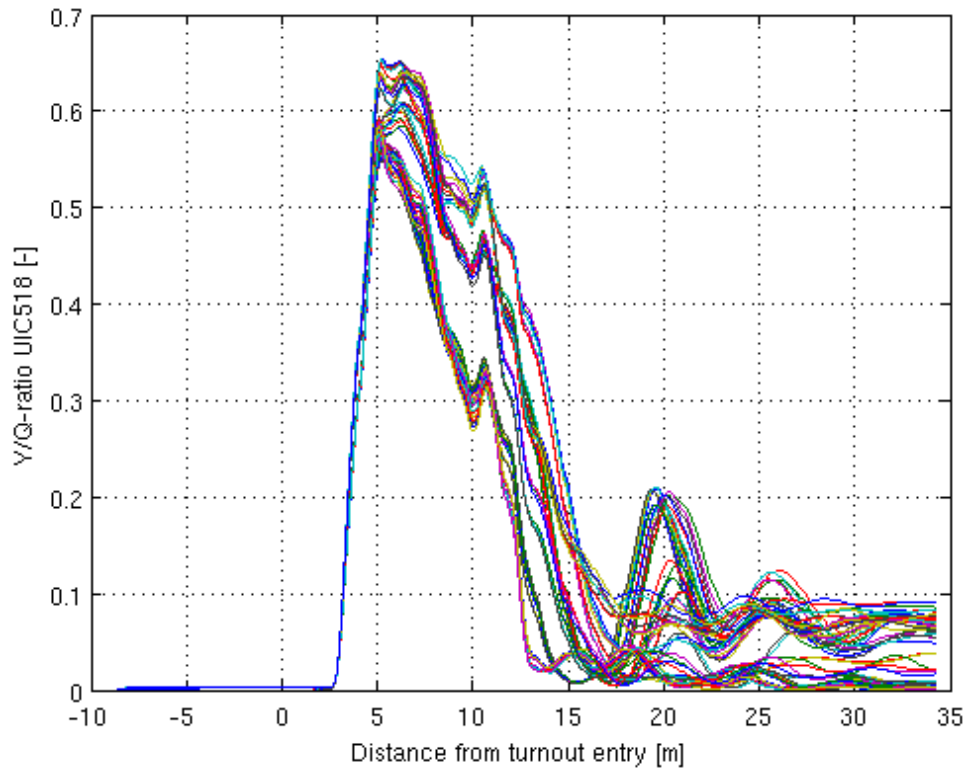


Figure 24 Y/Q-ratio from all the runs in setup one. The setup for these runs is described in Figure 25.

### 5.1.2 Result from setup 1

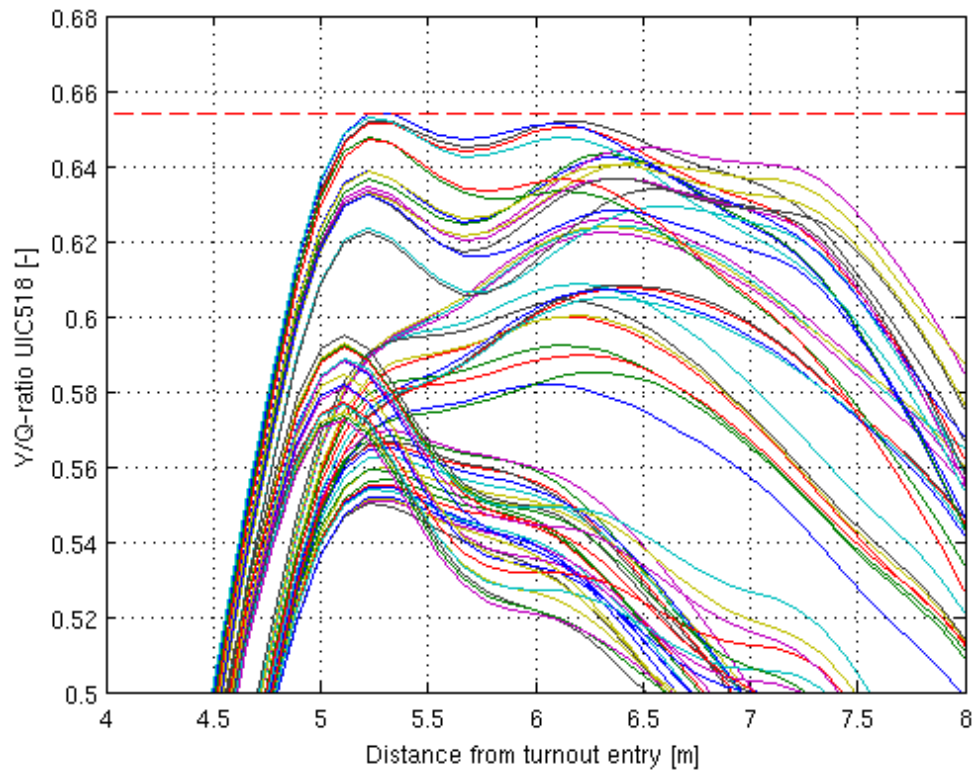


Figure 25 The resulting  $Y/Q$ -ratio from setup 1. The turnout in the simulation has a 760 metre radius, it is a unloaded (5 tonne) case and the nominal speed is set to 80 km/h. The maximum  $Y/Q$  value is 0.65 obtained approximately 5.25 metres into the turnout.

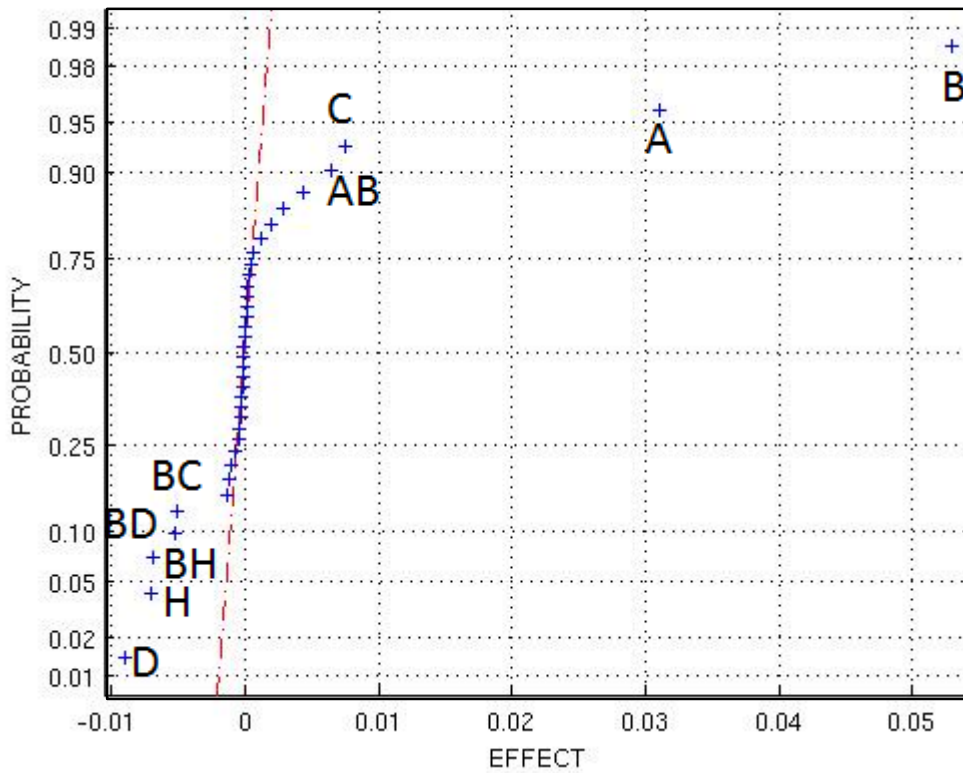


Figure 26 Setup one, curve radii 760m, unloaded (5 tons), speed 80km/h. The main effects, A, B, C, D and H have the largest values. Four two-way interactions with the largest effects are: AB, BH, BD and BC

For run number one, Figure 26 shows that the effects from factors B and A, friction coefficients for the sidebearer and the primary suspension damping surfaces, have the greatest effects, in the same order. Other main factors with large effects are H, C and D. BD and BH, are two-way interactions that show the largest effects. The interaction AB is between the friction coefficients of the primary suspension and the sidebearers. BH is the interaction between the friction coefficient for the sidebearers and the load distribution.

### 5.1.3 Result setup 2

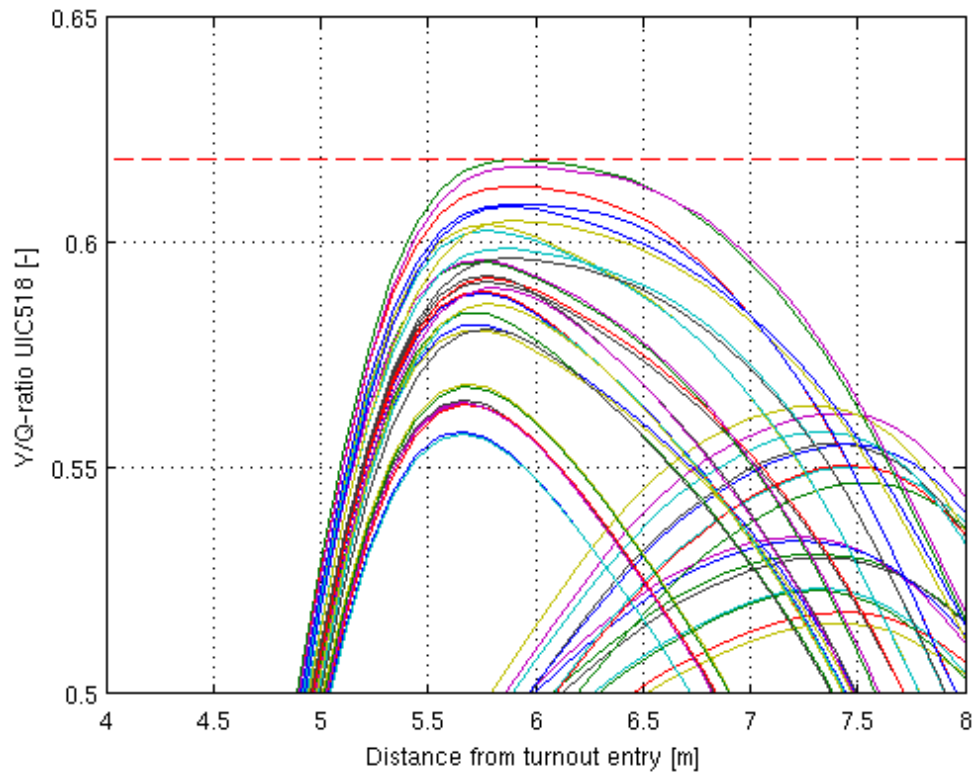


Figure 27 Plot that shows the runs from setup 2. The turnout in the simulation has a 760 metre radius, loaded (25 tonne) and the nominal speed is set to 80 km/h. Maximum Y/Q value is 0.62 obtained approximately 5.8 metres into the turnout.

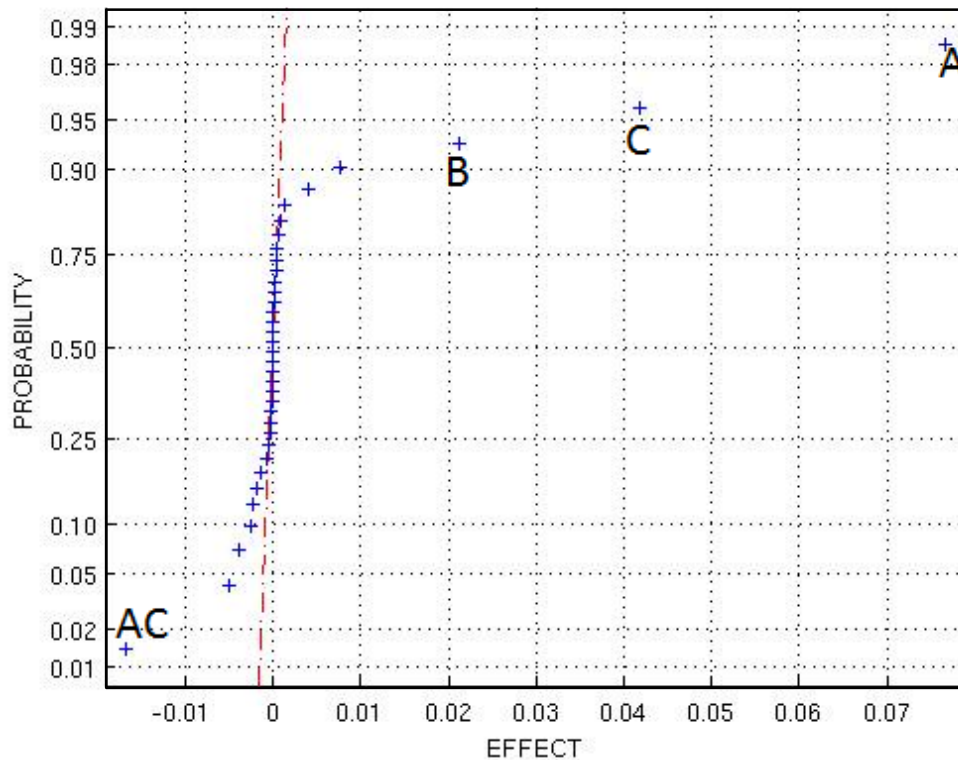


Figure 28 Setup two, curve radii 760m, loaded (25 tonnes), speed 80 km/h. Main effects with the highest values: A, B, and C, only one two-way interaction AC with a large effect.

The only changed setting for the second run is the load case which is changed from the tare case to the laden case, 25 tons. The order of the largest effects change from B-A-C to A-C-B. The interaction effect, AC, between the friction coefficient of the damping surfaces in the primary suspension and the centre pivot is the only interaction with large effect.

### 5.1.4 Result setup 3

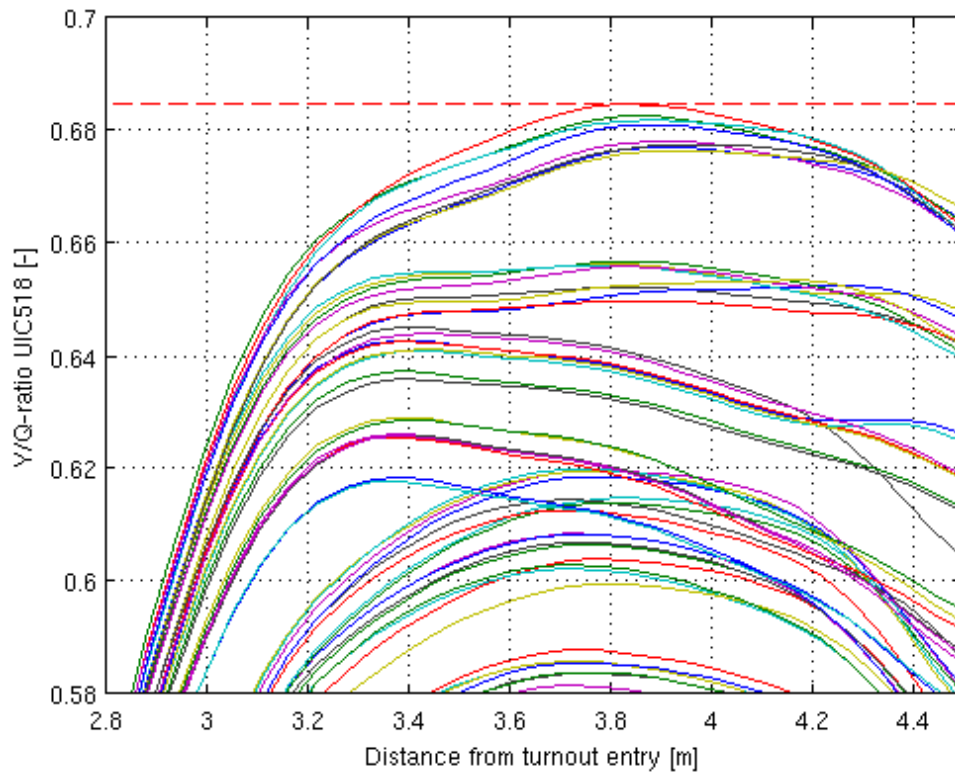


Figure 29 Plot that shows the runs from setup 3. The turnout in the simulation has a 190 metre radius, unloaded (5 tonnes) and the nominal speed is set to 40 km/h. The maximum Y/Q value for run 3 is 0.69 approximately 3.82 metres into the turnout.

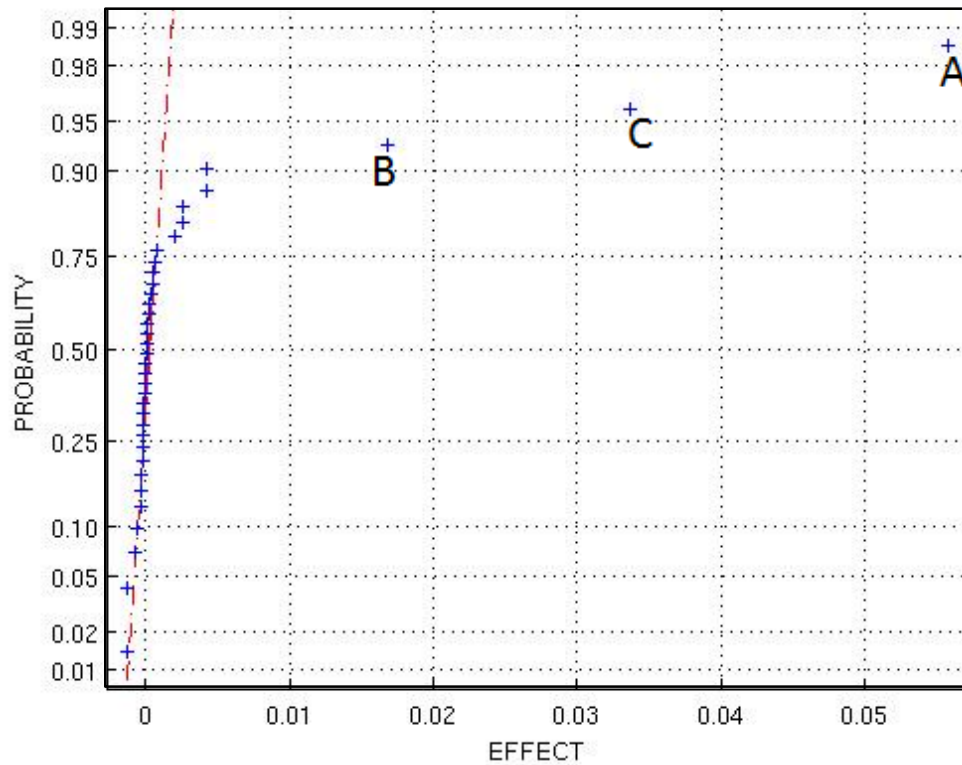


Figure 30 Setup three curve radii 190 m, loaded (25 tonnes), speed 40 km/h. Only the main factors have large effects: A, B and C.

In the third run, the radius is changed to 190 metres, the load is changed to the tare case and the speed is set to 40 km/h. The largest effects come from the changes of the main factors: A, B, C and H but also from the two-way interactions AB and BH. Compared with the first run the order of main effects is the same.

### 5.1.5 Result setup 4

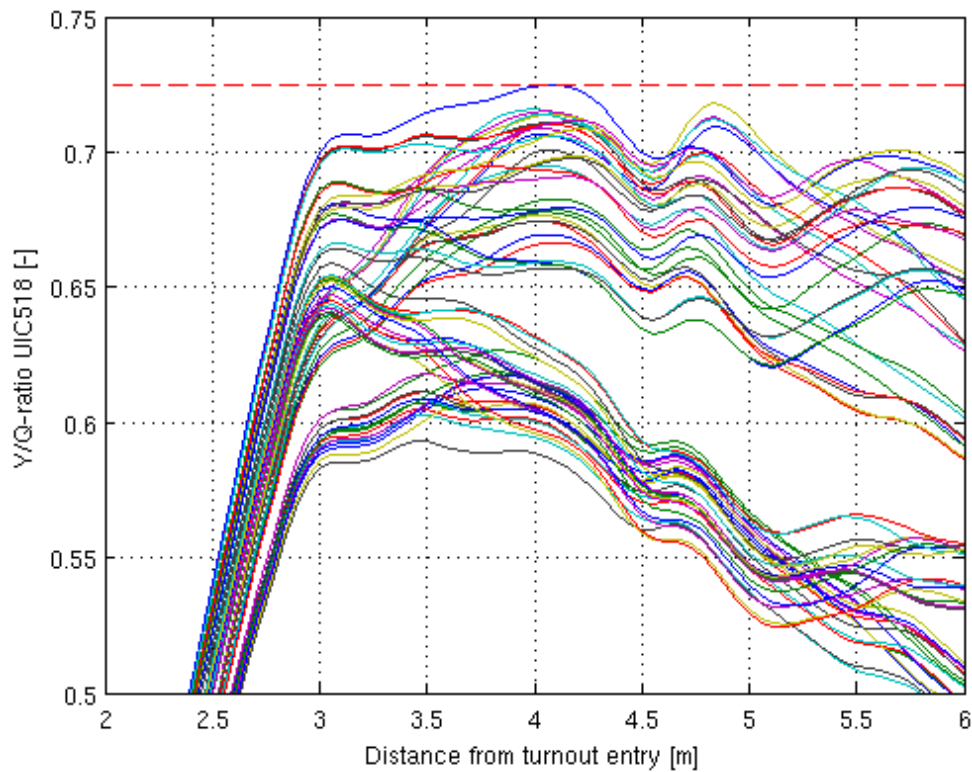


Figure 31 Plot that shows the runs from setup 4. The turnout in the simulation has a 190 metre radius, loaded (25 tonnes) and the nominal speed is set to 40 km/h. Maximum Y/Q value for run 4 is 0.73 approximately 4.2 metres into the turnout.

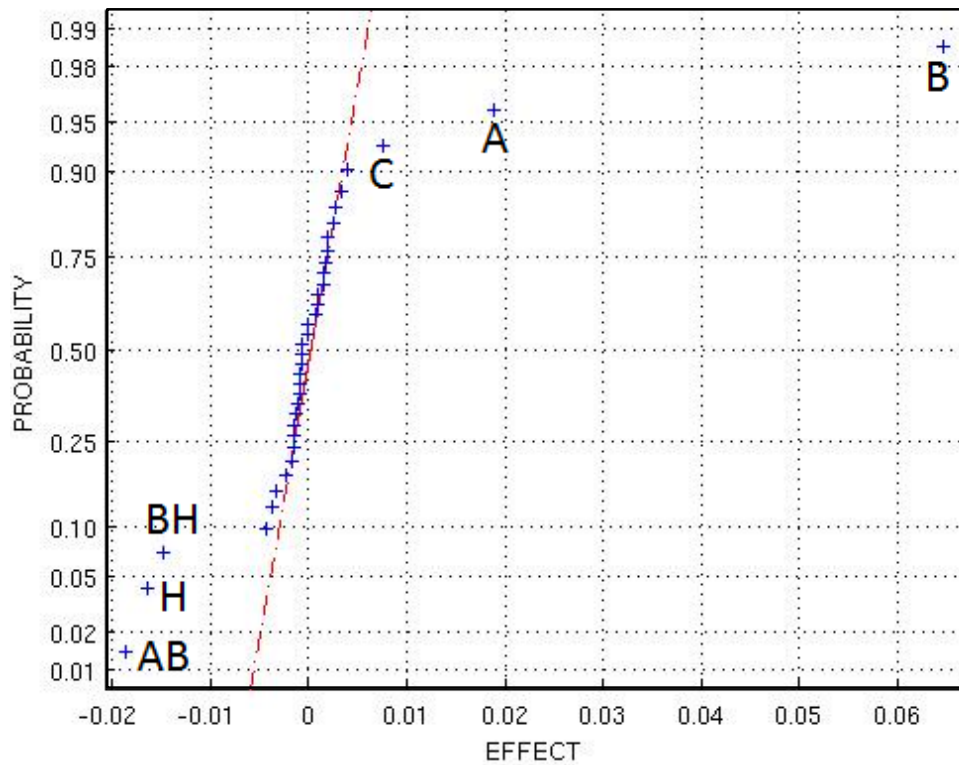


Figure 32 Setup four curve radii 190 m, unloaded (5 tonnes), speed 40 km/h. Main effects with large effects: A, B, C and H. Two interactions effects are large: AB and BH.

In run number four the order of the largest effects is the same as for run number two but the magnitudes of the values are reduced. The effect A is followed by C and then B. The value of the largest effect, A is smaller than in run number two. It is noticed that the interaction effect AC is not showing any significance in this run.

It can be seen from the normplots (figures 3-6 above) that the factors A, B, C and D repeatedly shows significance, even H has a large effect in two setups. The same factors that are connected to these effects also appear in two-way interactions. These five factors are selected for continued investigation in DOE 2, which focuses on the response from a larger amount of parameters.

## 5.2 Conclusions DOE 1

From the two first plots, the following conclusions are drawn. In setup one, representing a 760 meter radius curve with the car in its tare case at a speed of 80 km/h, changes of the main factors A, B, C and H together with the two-way interactions BC, BD and BH give the greatest effects. The maximum  $Y/Q$ -ratio value: 0.65

In the second run, similar to the first run except that it is the laden case, changes of the main factors A, B and C and the interaction AC gives the largest effects. The maximum  $Y/Q$ -ratio value is 0.62. The effect pattern for the tare and laden cases will change depending on the load. The load is significant and is included in DOE 2 together with the factor H, load distribution, also connected to the load case.

In the third run, tare case, the turnout is changed to a 190 metre radius and the speed is set to 40 km/h. The factors with the greatest effects are A, B, C and H. The two interactions AB and BH also have large effects. The maximum  $Y/Q$ -ratio value is 0.69.

In the fourth run, a laden case simulation, only changes of the three main factors A, B and C show significance. This run shows the same order of the effects except for the AC interaction that does not appear. The maximum  $Y/Q$ -ratio value is 0.73.

**Table 8 Maximum  $Y/Q$ -ratio for the four runs in the DOE 1, the largest value is obtained for run 4 with a  $Y/Q$ -ratio of 0.73.**

Run	Maximum $Y/Q$ -ratio
#1	0.65
#2	0.62
#3	0.69
#4	0.73

This experiment shows that the factors A, B, C, D and H are the factors that contribute the most to the  $Y/Q$ -ratio and they are therefore of interest for further investigation in DOE 2. The change of the turnout radius as a parameter is excluded in the next experiment even though it is considered significant. The largest value of the  $Y/Q$ -ratio is obtained for the 190 metre curve radius and therefore this turnout radius will be used for further investigations.

## 6 DOE 2

Besides the increased number of factors, fourteen instead of eight, the methodology is the same for the DOE 2 as for the DOE 1. The Matlab script is parameterized to meet variations in the DOE matrix and in the evaluation process. The computational time cost for a 256 run experimental design is about five hours. A shorter description of the 14 parameters and their high and low values can be seen in Table 9. These parameters are controlling the vehicle, the track and the bogie design. The wheel- rail friction coefficient, the nominal speed and the centre of gravity is held at constant values.

Table 9 DOE 2 containing 14-parameters.

Factor	Description	Low level	High level
A:	Friction coefficients for primary suspension	0.1	0.5
B:	Friction coefficient for side bearers	0.1	0.5
C:	Friction coefficient for centre	0.1	0.5
D:	Play: distance between side bearer friction surface and boarders	0.5[mm]	1[mm]
E:	Axle load, tare or laden case	5[tons]	25[tons]
F:	Bogie C-C distance	7000[mm]	15700[mm]
G:	Wheel profile	S1002(nominal)	Hollow worn
H:	Load distribution between side bearer and centre pivot*	0.28/0.75[%]	0.48/0.95[%]
I:	Suspension stiffness, standard or nominal	Standard	Nominal*100
J:	Suspension tweak – standard or diagonally changed preload	Standard	Tweaked
K:	Gauge distance	1435[mm]	1425[mm]
L:	Twisted track	Nominal	Twist
M:	Hanging sleeper	Fixed	Hanging
N:	Turnout entry	Tangential	Radial

\*If the run is made as a tare case (5 tonnes) the low and high levels of the load distribution between centre pivot and sidebearer are set to 28% and 48% respectively. In the loaded case, the low and high levels are set to 0.75% and 0.95%.

### 6.1 Results DOE 2

For the final setup the most critical radius and velocity combination is used: 190 metre radius with the speed set to 40 km/h. The  $Y/Q$ -ratio reaches 1.346 about 3.4 metres into the turnout. These values correspond to run number 145 in the DOE and the settings for that specific run can be seen in Table 10.

### 6.1.1 Result setup 5

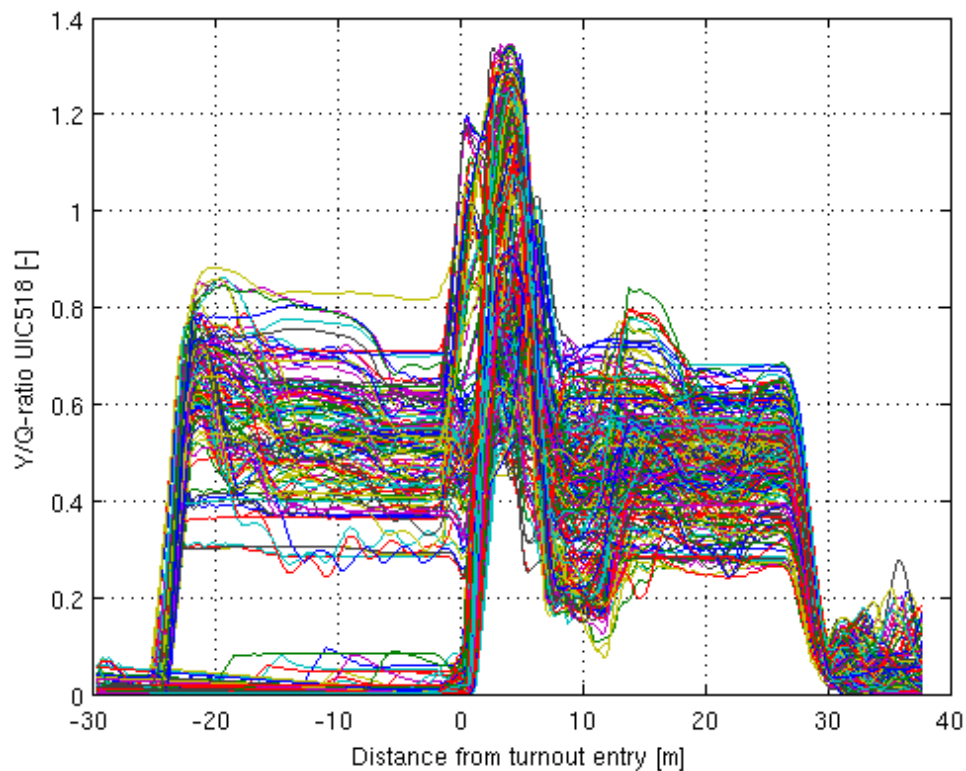


Figure 33.  $Y/Q$ -ratio result from the 256 runs in setup 5

The resulting values of the  $Y/Q$ -ratio from the 256 runs are separated into two categories. The first cluster of increased  $Y/Q$ -ratio values, starting approximately 25 metres before the turnout (at -25 m), depends on the radial entry where the lateral forces grow as the vehicle negotiates the curve. The second  $Y/Q$ -ratio climb is due to the turnout entry (at 0 m), where the radial entry samples increase again and the tangential entry samples rise from about zero. After the peak at the switch toe the  $Y/Q$  ratio decreases and an almost constant value is obtained about 15 metres before the values settles again. Some dynamic behaviour can be observed at the end of the plot as the route becomes straight.

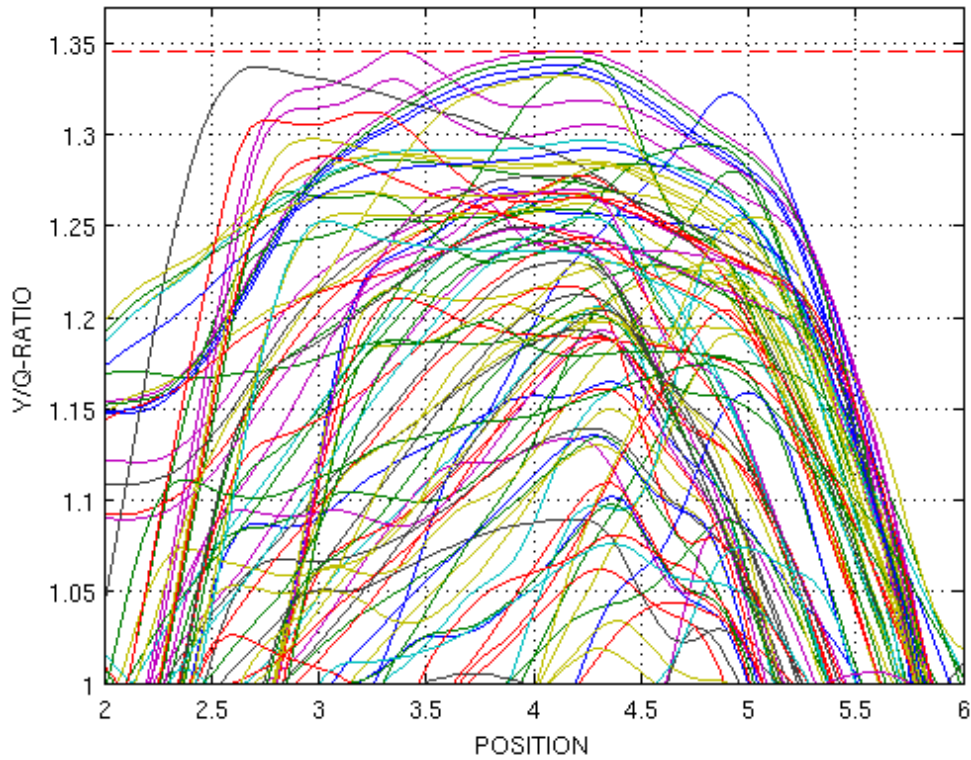


Figure 34 The 256 runs from setup 5. The turnout in the simulation has a 190 metre radius and the nominal speed is set to 40 km/h. The largest Y/Q values are zoomed in, the maximum value, 1.346, is obtained for run 145, 3.4 metres into the turnout.

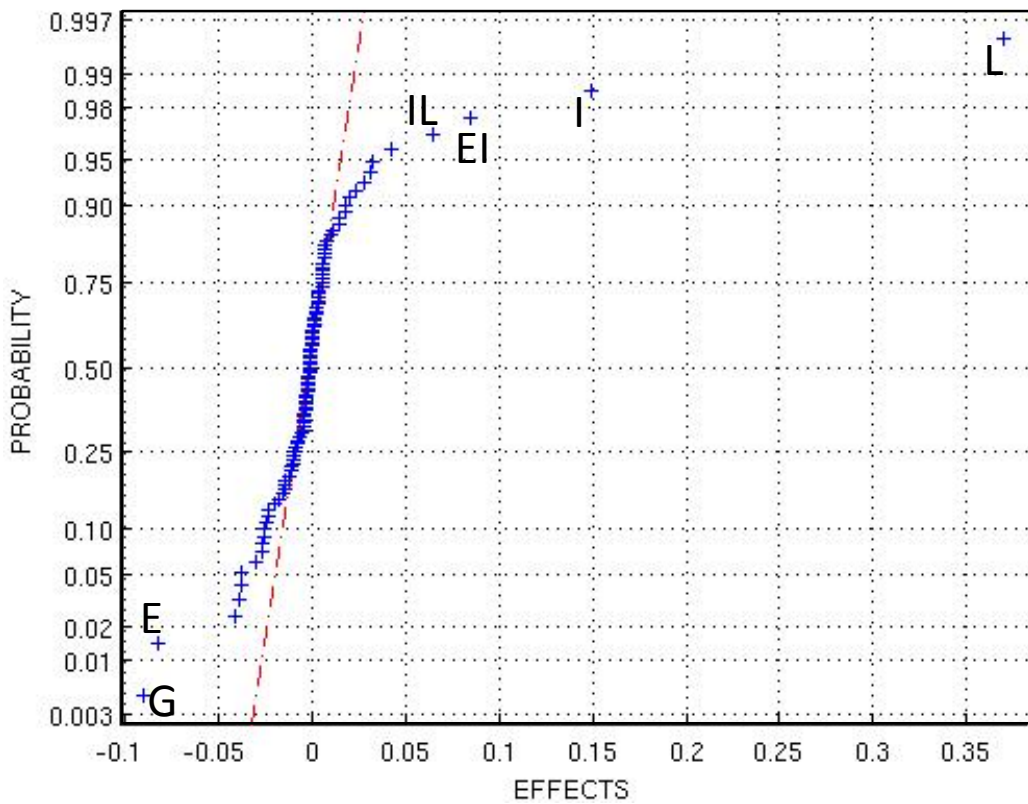


Figure 35. Normal probability plot of the effects from run 5, the main effects from factors L and I are most significant followed by E and G. two, two-way interactions EI and IL are also showing significance.,

From DOE 2 it is seen that the main factors: L, I, E and G have the most significant effects. The two-way interactions EI and IL also show significance. This means that track irregularities are the most significant for the  $Y/Q$ -ratio. The second most significant factor is the stiffness of the primary suspension. The third and fourth most significant main factors are the axle load and the wheel profile.

**Table 10.** The 14 parameters included in DOE 2 together with the values for the obtained worst case scenario.

Factor	Description	Level	Value
A	Friction coefficient primary suspension	High	0.5
B	Friction coefficient sidebearers	Low	0.1
C	Friction coefficient centre pivot	Low	0.1
D	Play	High	2=1[mm]
E	Axle load	Low	5[ton]
F	Bogie C-C distance	Low	3.5[m]
G	Wheel profiles	High	Hzdif4mm
H	Load distribution	High	0.48
I	Suspension stiffness	High	Frozen(*100)
J	Suspension tweak	Low	Skew
K	Gauge distance	Low	-0.01[mm]
L	Track	High	Twisted
M	Sleeper	High	Loose
N	Entry	High	Tangential

## 6.2 Conclusions

A parametric study of a railway vehicle, equipped with Y25 bogies, negotiating a turnout has been performed to quantify the effect different parameters have on derailment risk as evaluated by the  $Y/Q$ -ratio. In total 17 parameters were examined in two separate designs of experiments. An initial DOE with eight vehicle based parameters was used to screen out three parameters controlling the stiffness in the centre pivot which did not show any significance to the  $Y/Q$ -ratio.

Three parameters control the friction coefficients for the damping surfaces in the centre pivot and in the primary and secondary suspensions. The remaining two controls the play in the sidebearers and the load distribution between the centre pivot and the sidebearers. These five significant factors are included together with additional nine parameters in the 14 parameter DOE 2.

It is shown that the effects from four main parameters, I, L, E and G (see Table 9) have the largest significance for the  $Y/Q$ -ratio of the vehicle when it is negotiating a UIC E160 190 1:9 turnout with a tangential entry at a speed of 40 km/h. The track irregularity (track twist) represented by a dip has the highest influence on the  $Y/Q$ -ratio. Two two-way interactions are showing significance. The most important combination is the interaction between the axle load and the primary suspension stiffness.

These results should be considered as guidelines as no verification is made to real physical measurements. The results are most likely qualitatively correct but the exact derailment limit is hard to quantify.

In TCRP report 71 [10], it is stated that derailment of wagons with re-profiled wheels have been observed in yards with low speed velocities. This is in contradiction to the

results achieved in this project, but could be explained by the sharp “edges” in the surface of the re-profiled wheel due to the lathing, which is not accounted for in the GENSYS model.

## 7 Derailment limit

As mentioned in Section 6, the parameters regarding the surrounding environment are held constant during the DOE controlled simulations. They are already known to have a critical impact on the  $Y/Q$ -ratio and the derailment risk.

Example: -a high wheel-rail friction coefficient will affect the  $Y/Q$ -ratio and increase the risk for derailment. Speeds above the speed limit will also have a negative effect as the train negotiates a curve or turnout. A speeding train is probably explained by a human mistake or human action. A poorly placed cargo can also be due to a human error.

In order to find the limits for these parameters, an additional experiment has been performed using the worst case scenario setup as obtained in the DOE 2. It is here used to investigate the  $Y/Q$ -ratio dependency of three surrounding parameters; the wheel-rail friction coefficient, the nominal speed and the Centre Of Gravity (COG). The speed and the friction coefficient are varied while the centre of gravity is located at ten different locations around the carbody, see Figure 36. The COG locations that were used in order to find the worst case scenario. Positions 1, 2, 5 and 6 are above the leading bogie. Two locations, 4 and 8, are highlighted in the picture. These locations indicate the most critical positions for the COG of the displaced cargo. The best locations, with no derailment, are 2 and 6 which are the locations closest to the front left wheel of the first bogie.

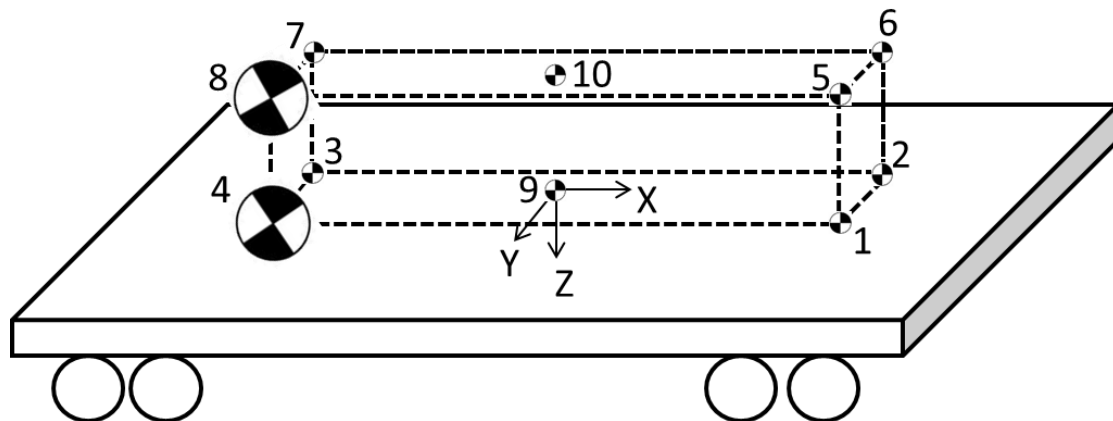


Figure 36 A schematic picture of the different.

In this derailment-limit-experiment the same turnout, 60E1-190-1:9, is used as in the earlier DOE's. It is a right turn turnout and the coordinate system is located at the centre of the carbody where the X-axis has positive coordinates in the facing direction of the train. The Y-axis is the lateral coordinate, positive in the right direction and the Z-axis is the vertical coordinate, positive in downwards direction.

Table 11 Centre of gravity positions.

Centre of gravity positions			
COG	X[m]	Y[m]	Z[m]
1	2.08	-0.1	2
2	2.08	0.1	2
3	-2.08	-0.1	2
4	-2.08	0.1	2
5	2.08	-0.1	2.8
6	2.08	0.1	2.8
7	-2.08	-0.1	2.8
8	-2.08	0.1	2.8
9	2.08	-0.1	2
10	2.080	0.1	2.8

The COG positions are obtained from Green Cargo [14]. It is stated that the lateral displacement of the COG of the load should not deviate more than (+/-) 10 centimetres from the centre between the two wheels if the limit value of a fully loaded wagon is not to be breached.

The longitudinal COG position is calculated, also from [14], by limiting the axle load to 16 tonnes, so it is possible for the vehicle to travel on “grid A” of the Swedish railways. In Sweden, the COG of the load is not allowed to be high than 2.8 metres from the top of the rail. This is thus the max value in the negative Z-direction. The derailment criterion is set to a flange climb of the wheel larger than or equal to 10 millimetres. The interval for the friction coefficient and speed are shown in Table 8.

Table 12 The interval for the friction coefficient between the wheel and the rail together with the interval for the vehicle speed.

Friction coefficient[-]	velocity
0.3	40
0.4	42
0.5	44
0.6	46
0.7	48
0.8	50
0.9	52
1.0	54
1.1	56

## 7.1 Derailment limit results

It is seen in Figure 38 that the worst position for the COG of the cargo load are the location points 4 and 8. These have a similar risk for derailment evaluated in terms of wheel flange climb. The positions are located above each other at the rear, inner right corner of the carbody (the train negotiates a right hand turnout). In Figure 37, the locations for points 2 and 6 show the best COG positions in terms of low derailment

risk. They are located above each other at the outer “corner” closest to the outer front left wheel.

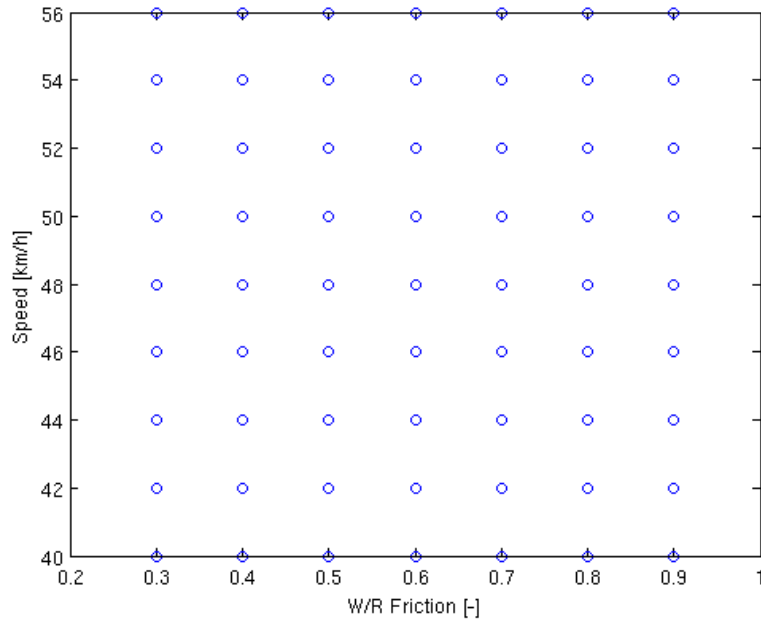


**Figure 37 . Flange climb derailment criterion evaluated for COG position 6. At this position and also at position 2, no derailment occurred as indicated by blue circles.**

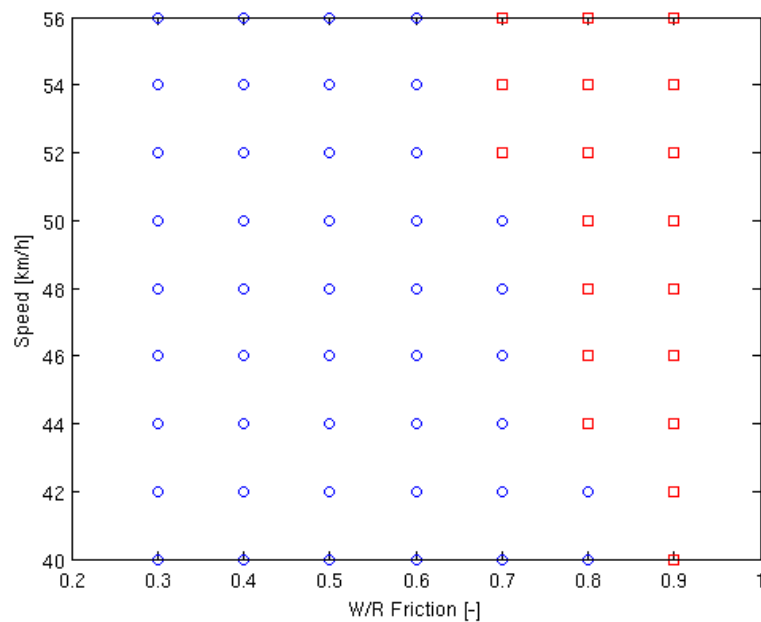


**Figure 38 . Flange climb derailment criterion evaluated for COG position 8. Combinations of speed and friction coefficient leading to high risk of derailment are shown as red squares in the plot.**

The result plots for points 4 and 8 are identical, which is also the case for points 2 and 6. However the resolution of the parameters is coarse and finer steps could reveal a different pattern between the two.

## 7.2 Derailment limit conclusions

The results indicate that the location of the COG of the payload is an important factor for derailment. The worst case scenario is when a load is placed on the rear, right side of the vehicle as it is negotiating a right hand turnout. This will unload the front left

wheel, resulting in smaller vertical forces which will give a larger  $Y/Q$ -ratio and cause flange climbing. In an opposite fashion, if the load is located close to the front wheel, the vertical forces are increased which will prevent the flange from climbing.

This is a factor even more important than the 0.8 metre difference of the height of the COG. It is not likely for the friction coefficient to reach as high as 0.8 and 0.9 and therefore it is more interesting to look at the variation of the speed. At speeds about 52km/h it can be seen that the friction coefficient between the wheel and the rail leading to risk of derailment can be lower, 0.7. It can be discussed how high speeds that should be included in the experiment as human errors always will be an important factor to the derailment risk. The extra weight on the rear bogie, as a result from the dislocated load, will probably give a larger wheel unloading in combination with the track dip.

## 8 Future work

To examine the  $Y/Q$ -ratio behaviour and be able to verify the results from this work, it would be necessary to perform a field test, evaluating the worst case settings obtained from the simulations. Further, a three level design of experiment could be investigated to reveal non-linear behaviour of the  $Y/Q$ -ratio from changes of the parameters.

A more thorough investigation of the derailment risk could be performed, for example by applying smaller speed steps and larger displacement of the COG of the payload. Measurements of the friction coefficient between wheel and rail would be useful in order to set better boundaries in the derailment experiments.

## 9 Sustainable development

There is a discussion around the world today about our environment. The human society's enormous dependency of energy is threatening every life form on the planet. A lot of energy is consumed through freight transportation.

On land one of the most energy efficient transportation methods is by train. I personally think that the government in Sweden today makes a big mistake when they neglect the maintenance and expansion of the railroad. Great investments in planning and developing the infrastructure are necessary. I am convinced that in the future, transportation by trains will be much more common for both people and freight.

Besides environmental and economic aspects, considering transportation methods, the combination of heavy duty trucks and small family cars on the same roads will always be a deadly hazard.

The low rolling resistance of train wheels on rails and the large load capacity of a, highly-efficient, electric locomotive makes train transportation competitive to any other land based transportation, considering energy-consumption/kg of transport.

In this thesis, simulations have been performed in order to quantify derailment risk which is necessary in order to be able to schedule maintenance and prevent accidents. This can contribute to reduce costs and make the railway transportation more cost effective as well as energy effective.

## 10 Bibliography

- [1] GENSYYS [www.gensys.se](http://www.gensys.se)[20120512]
- [2] N Wilson, R Fries, M Witte, A Haigermoser, M Wrang, J Evans and A Orlova, Assessment of safety against derailment using simulations and state-of-the-art assessment methods, *Vehicle System Dynamics*, Vol 49, Number 7, 2011
- [3] U Blomqvist, Försöksplanering - Faktorförsök, *Matematiklitteratur*, 2003
- [4] G E P Box, J S Hunter and W G Hunter, *Statistics for experimenters 2<sup>nd</sup> edition*, John Wiley & Sons Inc., New Jersey, 2005
- [5] Andersson, E. Berg .M and Stichel, S., 2007, *Rail Vehicle Dynamics*. Stockholm: Royal Institute of Technology
- [6] T Jendel, Dynamic analysis of a freight wagon with modified Y25 bogies, M Sc thesis, Department of Vehicle Engineering, Royal Institute of Technology, Stockholm, Sweden, 87pp, 1997
- [7] J H Sällström, T Dahlberg, M Ekh and J C O Nielsen, 2004, State-of-the-art study on railway turnouts-dynamic and damage, Department of Applied Mechanics, Chalmers University of Technology, Göteborg, Sweden
- [8] B Pålsson, 2011, Towards Optimization of Railway Turnouts, Department of Applied Mechanics, Chalmers University of Technology, Göteborg, Sweden
- [9] <http://www.greencargo.com/sv/Godsvagnar/Start/Specialvagnar/> [251113]
- [10]TCRPreport71[http://onlinepubs.trb.org/onlinepubs/tcrp/tcrp\\_rpt\\_71v5.pdf](http://onlinepubs.trb.org/onlinepubs/tcrp/tcrp_rpt_71v5.pdf) [120406]
- [11] Kassa, E. Nielsen, J., 2007. Stochastic Analysis of Dynamic Interaction between Train and Turnout, paper D. Gothenburg: Chalmers University of Technology, Department of Applied mechanics
- [12] <http://www.itl.nist.gov/div898/handbook/pri/section5/pri594.htm> [120323]
- [13] <http://www.mathworks.se/help/toolbox/stats/fracfact.html> [201202-]
- [14][http://www.greencargo.com/Global/Kundservice%20jvg/Lastningsinfo/a\\_83-01%20riktlinjer.pdf](http://www.greencargo.com/Global/Kundservice%20jvg/Lastningsinfo/a_83-01%20riktlinjer.pdf) [120620]